CHAPTER – IV

SYNTHESIS, CHARACTERIZATION AND ANTIMICROBIAL ACTIVITY OF METAL CHELATES

CONTENTS

4.1 EXPERIMENTAL

The each ligands (TPAS-1 TO 5 and TPTB) was purified by dissolving in dilute alkali solution and reprecipitated by diluted HCL solution. All the ligands were processed up to dried amorphous powder state.

4.1.1 Preparation of Sodium Salt of Ligands

A purified and dried ligand sample (0.1 M) was mixed in 150 mL of acetone solvent and stirred. Aqueous molar NaOH solution (calculated amount) was added drop wise to the ligand solution. The thick solution was stirred for some hours till paste type precipitates appeared. A fixed quantity of water was added to make clear solution. The resulting solution was diluted to 250 mL water and this clear solution called as reagent solution. This aqueous solution was used for preparing metal chelates.

4.1.2 Synthesis of Metal Chelates of Ligands TPAS-1 to 5.

- **Chelates with Cu^{2+} Meatal ions:**

  25 ml of Na^{+} reagent solution of ligand (containing 10 mmol) was mixed dropwise to copper salt solution in 100 ml of deionized water, The pH of resultant mixture was adjusted by addition solid sodium acetate. A greenish – blue solid product was digested on boiling water bath for 2 hrs. It was filtered, washed by acetone and air -dried. The powder was dried in oven at 100^{o}C for a one day. The yield was 75%.

- **Chelates with Ni^{2+} Meatal ions:**

  25 ml of Na^{+} reagent solution of ligand (containing 10 mmol) was mixed dropwise to nickle salt solution in 100 ml of deionized water, The pH of resultant mixture was adjusted by addition solid sodium acetate. A wet cake product was digested on boiling water bath for 2 hrs. It was filtered, washed by acetone and air -dried. The powder was dried in oven at 100^{o}C for a one day. The yield was 72%.

- **Chelates with Co^{2+} Meatal ions**

25 ml of Na^{+} reagent solution of ligand (containing 10 mmol) was mixed dropwise to cobalt salt solution in 100 ml of deionized water, The pH of resultant mixture was adjusted by addition solid sodium acetate. A solid floppy material was digested on boiling water bath for 2 hrs. It was filtered, washed by acetone and air -dried. The powder was dried in oven at 100^{o}C for a one day. The yield was 66%.

- **Chelates with Mn^{2+} Meatal ions:**

25 ml of Na^{+} reagent solution of ligand (containing 10 mmol) was mixed dropwise to manganese salt solution in 100 ml of deionized water, The pH of resultant mixture was adjusted by addition solid sodium acetate. A wet cake product was digested on boiling water bath for 2 hrs. It was filtered, washed by acetone and air -dried. The powder was dried in oven at 100^{o}C for a one day. The yield was 75%.

- **Chelates with Zn^{2+} Metal Ions:**

25 ml of Na^{+} reagent solution of ligand (containing 10 mmol) was mixed dropwise to zinc salt solution in 100 ml of deionized water, The pH of resultant mixture was adjusted by addition solid sodium acetate. A wet cake product was digested on boiling water bath for 2 hrs. It was filtered, washed by acetone and air -dried. The powder was dried in oven at 100^{o}C for a one day. The yield was 67%. The dried chelate was pale yellowish powder.

4.1.3 Elemental analysis of metal chelates.

The elemental contents i.e. C, H, N and S elements of metal chelates were analyzing on elemental analyzer (Model: Thermofiniggan Flash 1101 EA). The results of analysis are described in Tables 4.1 to 4.4. It indicate that the result are consistent with the structure shown in scheme 4.1.

4.2 METAL: LIGAND (M:L) RATIO

Metal % in chelate was estimated by literature prcoedure[1]. In this process fix amount of ligand was taken in an evaporating dish and each one ml of Analar Concentrated HCL, H_2SO_4, and $HCLO_4$ were added. Then decompose the sample by evaporated to dryness. The residue was dissolved in distilled water and diluted to mark. The position of this solution was titrated against ethylenediamine tetra acetic acid (EDTA) solution and the metal % in chelate calculated. The results are mentioned in Table 4.1 to 4.6. The results indicate that Metal: Ligand (M:L) ration is 1:2 tor bivalent metals.

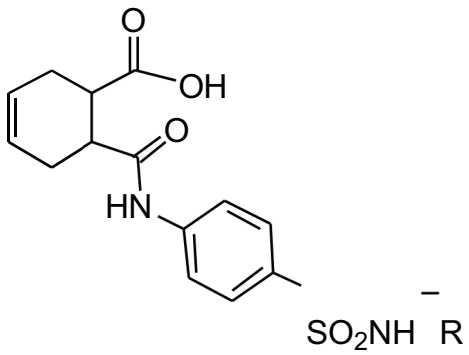

Ligands

Metal Acetate

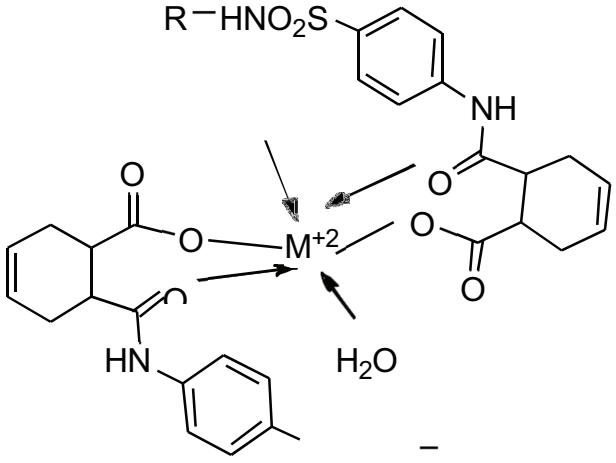

Metal cheltes of TPAS-1 to TPAS-6

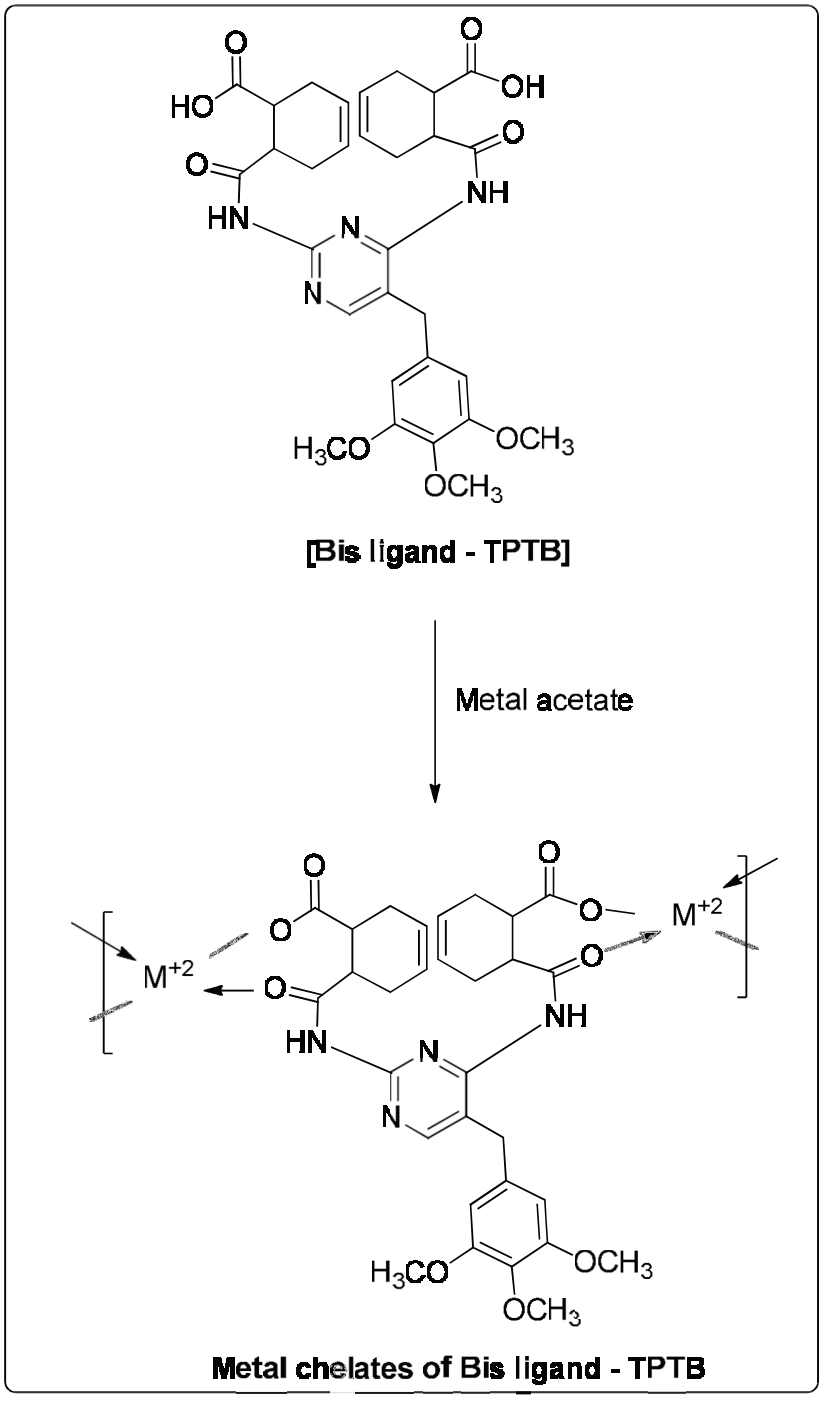
HO
O
O
OH
O
NH
HN
N
N
H3CO
OCH3
OCH3
[Bis ligand - TPTB]
Metal acetate
M+2
M+2
Metal chelates of Bis ligand - TPTB

4.3 ELEMENTAL ANALYSIS

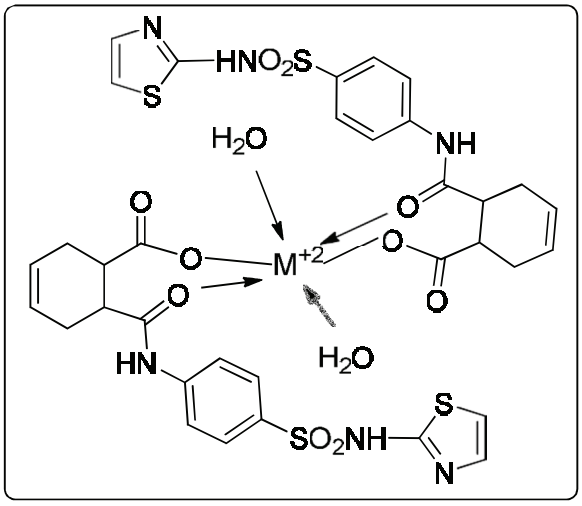

Metal chelates of ligand TPAS-1

Table 4.1: Properties of metal chelates of ligand TPAS-1

Metal Chelates	Molecular Formula	M.Wt.	Yield (%)
(TPAS-1)2 Cu^{2+}	C34H32N6O10S4 Cu^{2+}.2H2O	912.45	74
(TPAS-1)2 Ni^{2+}	C34H32N6O10S4 Ni^{2+}.2H2O	907.62	73
(TPAS-1)2 Mn^{2+}	C34H32N6O10S4Mn^{2+}.2H2O	903.92	76
(TPAS-1)2 Co^{2+}	C34H32N6O10S4 Co^{2+}.2H2O	907.92	68
(TPAS-1)2 Zn^{2+}	C34H32N6O10S4 Zn^{2+}.2H2O	914.32	66

Metal Chelates	% Metal Analysis		Elemental Analysis							
			%C		%H		%N		%S	
	Cald.	Found	Cald.	Found	Cald.	Found	Cald.	Found	Cald.	Found
$(TPAS\text{-}1)_2\,Cu^{2+}$	6.96	7.00	44.71	44.70	3.94	3.90	9.21	9.20	14.02	14.00
$(TPAS\text{-}1)_2\,Ni^{2+}$	6.47	6.50	44.95	45.00	3.97	4.00	9.25	9.30	14.10	14.10
$(TPAS\text{-}1)_2\,Mn^{2+}$	6.08	6.10	45.13	45.10	3.98	4.00	9.30	9.30	14.16	14.20
$(TPAS\text{-}1)_2\,Co^{2+}$	6.50	6.50	44.83	44.80	3.96	4.00	9.25	9.30	14.09	14.10
$(TPAS\text{-}1)_2\,Zn^{2+}$	7.15	7.15	44.51	44.50	3.94	4.00	9.18	9.20	13.99	14.00

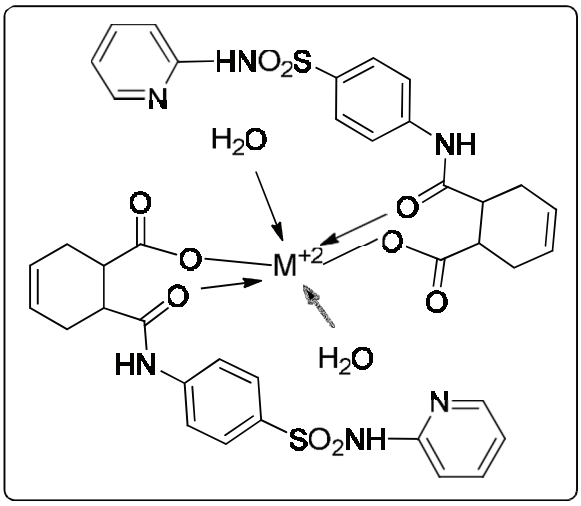

Metal chelates of ligand TPAS-2

Table 4.2: Properties of metal chelates of ligand TPAS-2

Metal Chelates	Molecular Formula	M.Wt.	Yield (%)
(TPAS-2)2 Cu^{2+}	C38H36N6O10S2 Cu^{2+}.2H2O	900.38	75
(TPAS-2)2 Ni^{2+}	C38H36N6O10S2 Ni^{2+}.2H2O	895.58	74
(TPAS-2)2 Mn^{2+}	C38H36N6O10S2 Mn^{2+}.2H2O	891.88	77
(TPAS-2)2 Co^{2+}	C38H36N6O10S2 Co^{2+}.2H2O	895.88	69
(TPAS-2)2 Zn^{2+}	C38H36N6O10S2 Zn^{2+}.2H2O	902.28	65

Metal Chelates	% Metal Analysis		Elemental Analysis							
			%C		%H		%N		%S	
	Cald.	Found	Cald.	Found	Cald.	Found	Cald.	Found	Cald.	Found
$(TPAS\text{-}2)_2\,Cu^{2+}$	7.05	7.00	50.64	50.60	4.44	4.40	9.33	9.30	7.10	7.10
$(TPAS\text{-}2)_2\,Ni^{2+}$	6.55	6.50	50.91	50.90	4.47	4.50	9.38	9.40	7.15	7.20
$(TPAS\text{-}2)_2\,Mn^{2+}$	6.16	6.20	51.12	51.10	4.48	4.50	9.42	9.40	7.17	7.20
$(TPAS\text{-}2)_2\,Co^{2+}$	6.58	6.60	50.90	50.90	4.46	4.50	9.37	9.40	7.14	7.10
$(TPAS\text{-}2)_2\,Zn^{2+}$	7.20	7.20	50.53	50.50	4.43	4.40	9.31	9.30	7.09	7.10

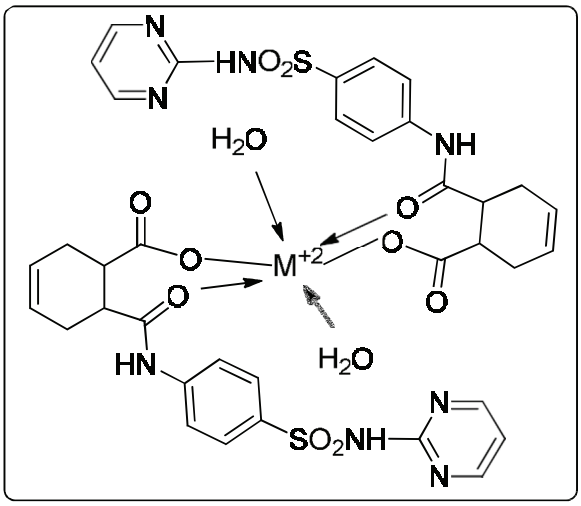

Metal chelates of ligand TPAS-3

Table 4.3: Properties of metal chelates of ligand TPAS-3

Metal Chelates	Molecular Formula	M.Wt.	Yield (%)
$(TPAS\text{-}3)_2\ Cu^{2+}$	$C_{36}H_{34}N_8O_{10}S_2\ Cu^{2+}.2H_2O$	902.34	76
$(TPAS\text{-}3)_2\ Ni^{2+}$	$C_{36}H_{34}N_8O_{10}S_2\ Ni^{2+}.2H_2O$	897.54	75
$(TPAS\text{-}3)_2\ Mn^{2+}$	$C_{36}H_{34}N_8O_{10}S_2\ Mn^{2+}.2H_2O$	893.84	76
$(TPAS\text{-}3)_2\ Co^{2+}$	$C_{36}H_{34}N_8O_{10}S_2\ Co^{2+}.2H_2O$	897.84	70
$(TPAS\text{-}3)_2\ Zn^{2+}$	$C_{36}H_{34}N_8O_{10}S_2\ Zn^{2+}.2H_2O$	904.24	66

Metal Chelates	% Metal Analysis		Elemental Analysis							
			%C		%H		%N		%S	
	Cald.	Found	Cald.	Found	Cald.	Found	Cald.	Found	Cald.	Found
$(TPAS\text{-}3)_2\,Cu^{2+}$	7.03	7.00	47.87	47.90	4.21	4.20	12.41	12.40	7.09	7.10
$(TPAS\text{-}3)_2\,Ni^{2+}$	6.54	6.50	48.13	48.10	4.23	4.20	12.48	12.50	7.13	7.10
$(TPAS\text{-}3)_2\,Mn^{2+}$	6.15	6.20	48.33	48.30	4.25	4.30	12.53	12.50	7.16	7.20
$(TPAS\text{-}3)_2\,Co^{2+}$	6.57	6.60	48.11	48.10	4.23	4.30	12.47	12.50	7.13	7.10
$(TPAS\text{-}3)_2\,Zn^{2+}$	7.23	7.20	47.77	47.80	4.20	4.20	12.38	12.40	7.08	7.10

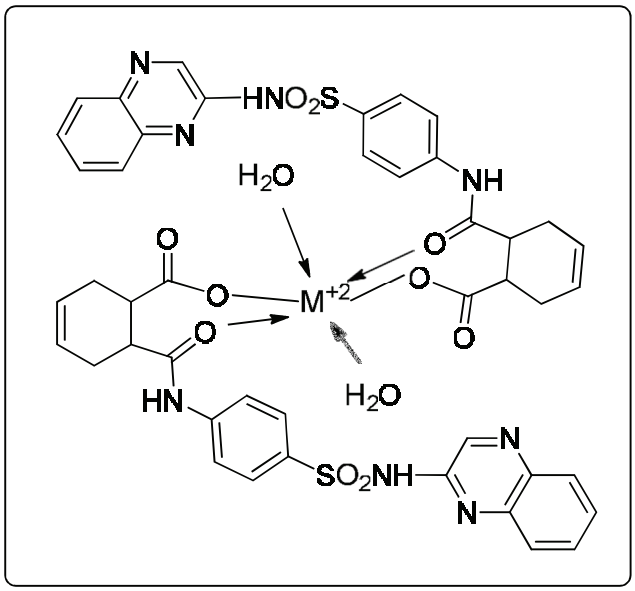

Metal chelates of ligand TPAS-4

Table 4.4: Properties of metal chelates of ligand TPAS-4

Metal Chelates	Molecular Formula	M.Wt.	Yield (%)
(TPAS-4)2 Cu^{2+}	C44H38N8O10S2 Cu^{2+}.2H2O	1002.46	75
(TPAS-4)2 Ni^{2+}	C44H38N8O10S2 Ni^{2+}.2H2O	997.66	77
(TPAS-4)2 Mn^{2+}	C44H38N8O10S2 Mn^{2+}.2H2O	993.96	75
(TPAS-4)2 Co^{2+}	C44H38N8O10S2 Co^{2+}.2H2O	997.96	72
(TPAS-4)2 Zn^{2+}	C44H38N8O10S2 Zn^{2+}.2H2O	1004.36	68

Sr. No.	Metal Chelates	% Metal Analysis		Elemental Analysis							
				%C		%H		%N		%S	
		Cald.	Found	Cald.	Found	Cald.	Found	Cald.	Found	Cald.	Found
1.	$(TPAS\text{-}4)_2\,Cu^{2+}$	6.33	6.30	52.67	52.70	4.19	4.20	11.17	11.20	6.38	6.40
2.	$(TPAS\text{-}4)_2\,Ni^{2+}$	5.88	5.90	52.72	52.70	4.21	4.20	11.23	11.20	6.41	6.40
3.	$(TPAS\text{-}4)_2\,Mn^{2+}$	5.53	5.50	53.12	53.10	4.23	4.20	11.27	11.30	6.44	6.40
4.	$(TPAS\text{-}4)_2\,Co^{2+}$	5.91	6.00	52.90	52.90	4.21	4.20	11.22	11.20	6.41	6.40
5.	$(TPAS\text{-}4)_2\,Zn^{2+}$	6.51	6.50	52.57	52.50	4.18	4.20	11.15	11.20	6.37	6.40

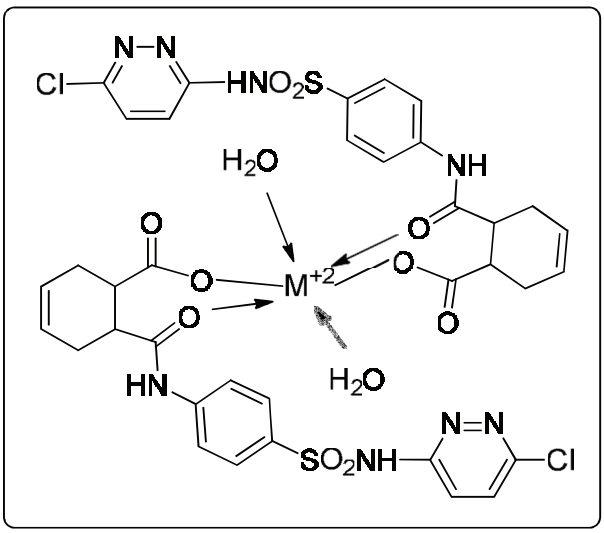

Metal chelates of ligand TPAS-5

Table 4.5: Properties of metal chelates of ligand TPAS-5

Metal Chelates	Molecular Formula	M.Wt.	Yield (%)
(TPAS-5)2 Cu^{2+}	$C_{36}H_{32}N_8O_{10}S_2Cl_2\ Cu^{2+}.2H_2O$	971.24	76
(TPAS-5)2 Ni^{2+}	$C_{36}H_{32}N_8O_{10}S_2Cl_2\ Ni^{2+}.2H_2O$	966.44	75
(TPAS-5)2 Mn^{2+}	$C_{36}H_{32}N_8O_{10}S_2Cl_2\ Mn^{2+}.2H_2O$	962.74	77
(TPAS-5)2 Co^{2+}	$C_{36}H_{32}N_8O_{10}S_2Cl_2\ Co^{2+}.2H_2O$	966.74	73
(TPAS-5)2 Zn^{2+}	$C_{36}H_{32}N_8O_{10}S_2Cl_2\ Zn^{2+}.2H_2O$	973.14	69

Metal Chelates	% Metal Analysis		Elemental Analysis							
			%C		%H		%N		%S	
	Cald.	Found	Cald.	Found	Cald.	Found	Cald.	Found	Cald.	Found
$(TPAS\text{-}5)_2\,Cu^{2+}$	6.54	6.50	44.48	44.50	3.70	3.70	11.53	11.50	6.59	6.60
$(TPAS\text{-}5)_2\,Ni^{2+}$	6.07	6.10	44.70	44.70	3.72	3.70	11.59	11.60	6.62	6.60
$(TPAS\text{-}5)_2\,Mn^{2+}$	5.71	5.70	44.87	44.90	3.74	3.70	11.63	11.60	6.65	6.60
$(TPAS\text{-}5)_2\,Co^{2+}$	6.10	6.10	44.68	44.70	3.72	3.70	11.58	11.60	6.62	6.60
$(TPAS\text{-}5)_2\,Zn^{2+}$	6.72	6.70	44.39	44.40	3.70	3.70	11.51	11.50	6.58	6.60

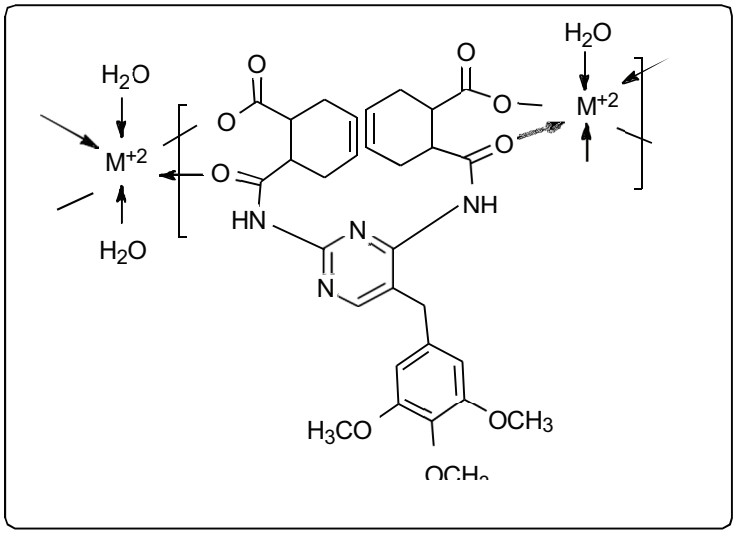

Metal chelates of Bis-ligand TPTB

Table 4.6: Properties of metal chelates of Bis-ligand TPTB

Metal Chelates	Molecular Formula	M.Wt.	Yield (%)
(TPTB)2 Cu^{2+}	$C_{60}H_{64}N_8O_{18}Cu^{2+}.2H_2O$	1284.72	75
(TPTB)2 Ni^{2+}	$C_{60}H_{64}N_8O_{18}Ni^{2+}.2H_2O$	1279.92	77
(TPTB)2 Mn^{2+}	$C_{60}H_{64}N_8O_{18}Mn^{2+}.2H_2O$	1276.22	74
(TPTB)2 Co^{2+}	$C_{60}H_{64}N_8O_{18}Co^{2+}.2H_2O$	1280.22	74
(TPTB)2 Zn^{2+}	$C_{60}H_{64}N_8O_{18}Zn^{2+}.2H_2O$	1286.62	68

Metal Chelates	% Metal Analysis		Elemental Analysis					
			%C		%H		%N	
	Cald.	Found	Cald.	Found	Cald.	Found	Cald.	Found
$(TPTB)_2\,Cu^{2+}$	4.94	5.00	56.04	56.00	5.29	5.30	8.71	8.70
$(TPTB)_2\,Ni^{2+}$	4.59	4.60	56.25	56.30	5.31	5.30	8.75	8.70
$(TPTB)_2\,Mn^{2+}$	4.31	4.30	56.41	56.40	5.33	5.30	8.77	8.80
$(TPTB)_2\,Co^{2+}$	4.60	4.60	56.24	56.20	5.31	5.30	8.74	8.70
$(TPTB)_2\,Zn^{2+}$	5.08	5.10	55.96	56.00	5.28	5.30	8.70	8.70

4.4 INFRARED SPECTROSCOPY

The selected IR scans of metal chelates are presented in Figs. 4.1 to 4.8.

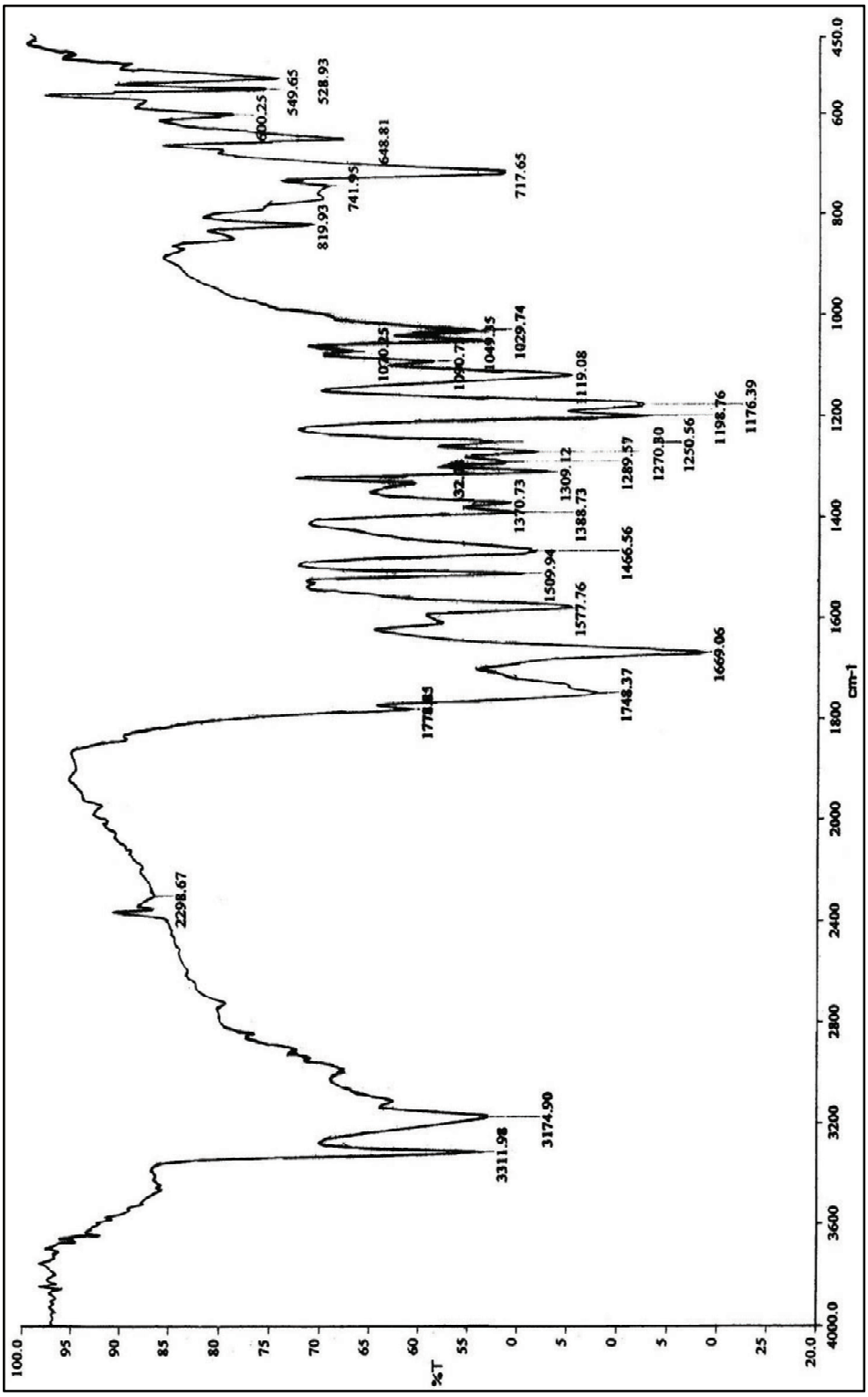

Fig. 4.1: IR spectrum of $[TPAS\text{-}1]_2\ Cu^{2+}$

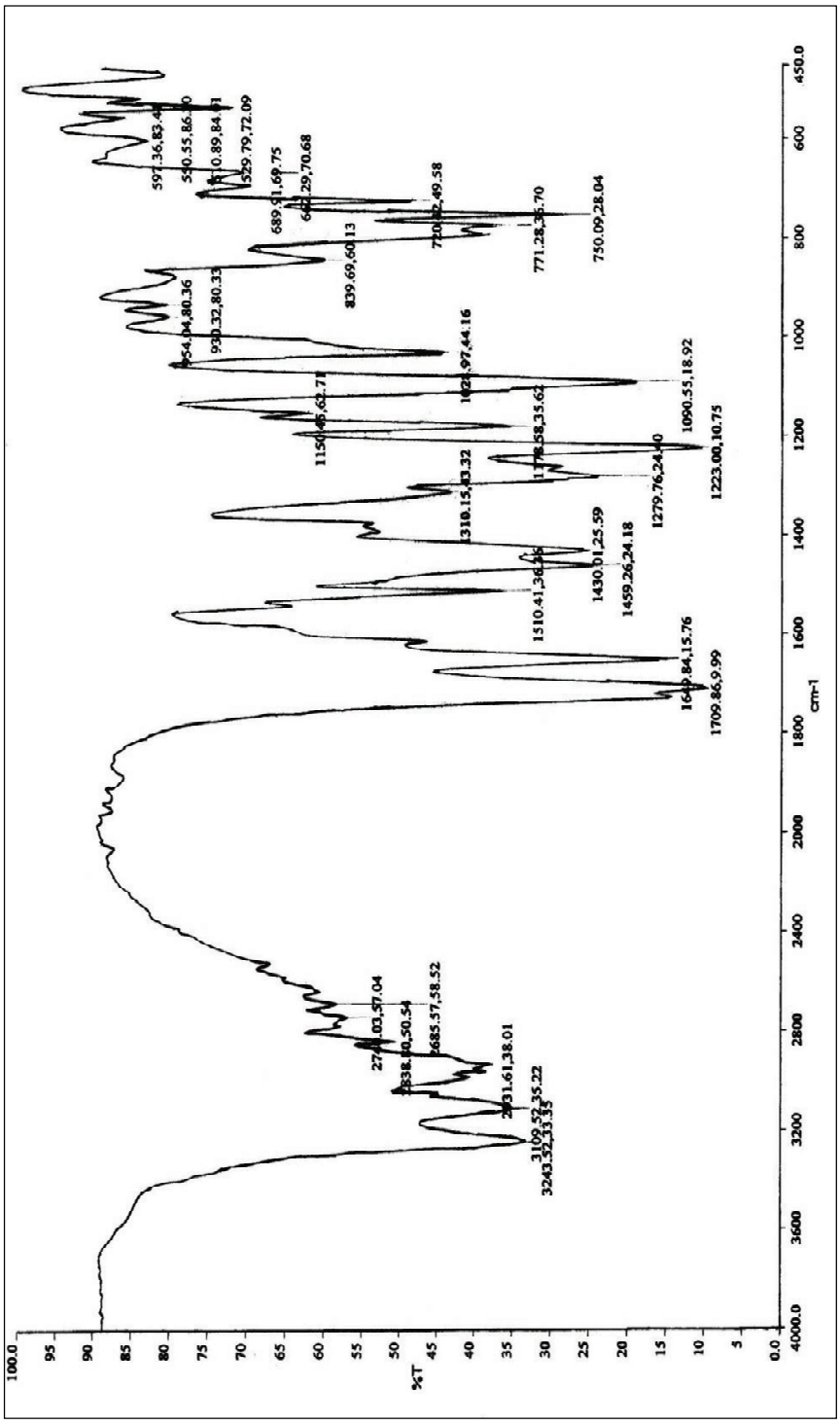

Fig. 4.2: IR spectrum of $[TPAS\text{-}1]_2Mn^{2+}$

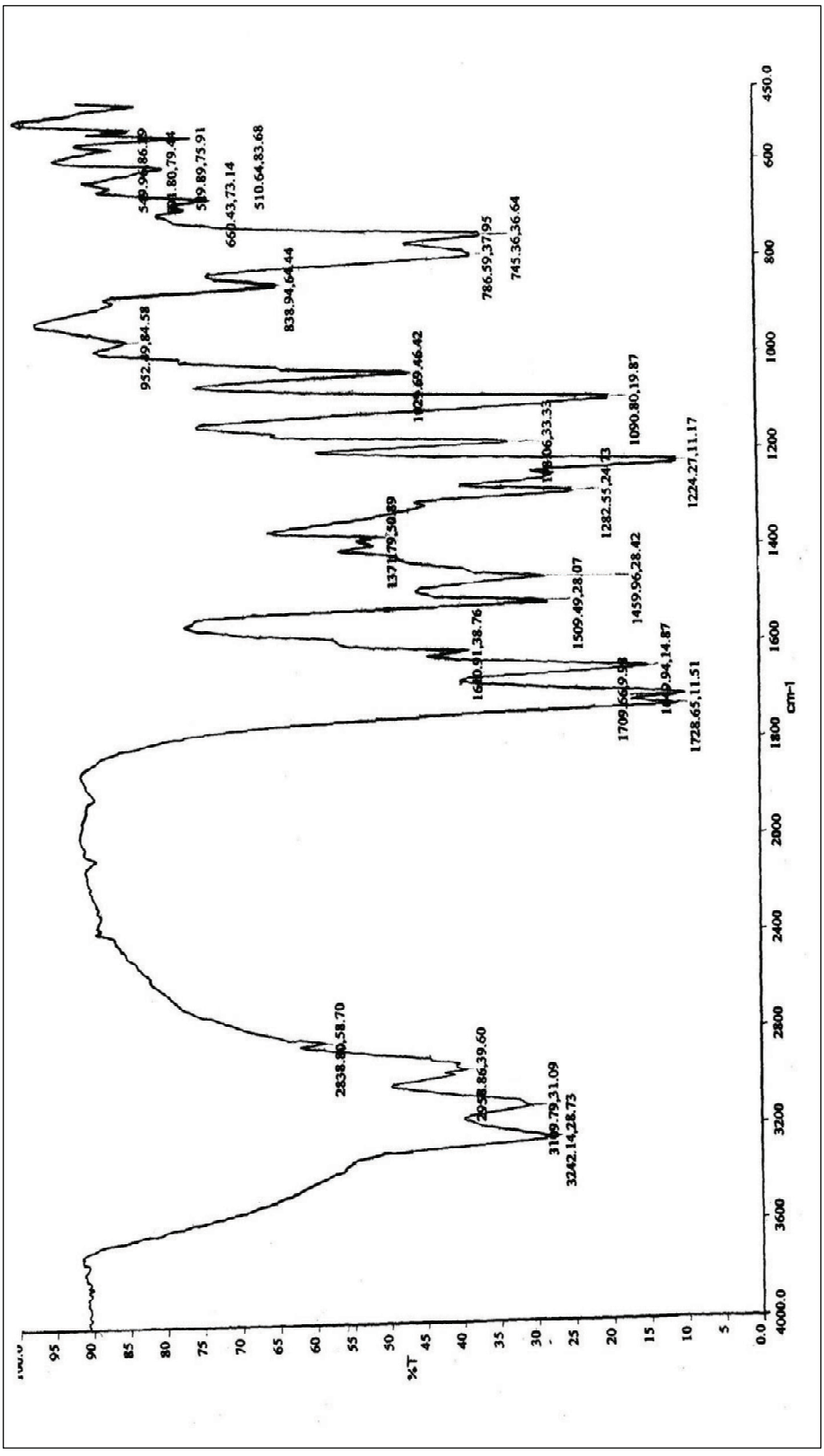

Fig. 4.3: IR spectrum of [TPAS-3]$_2$ Co^{2+}

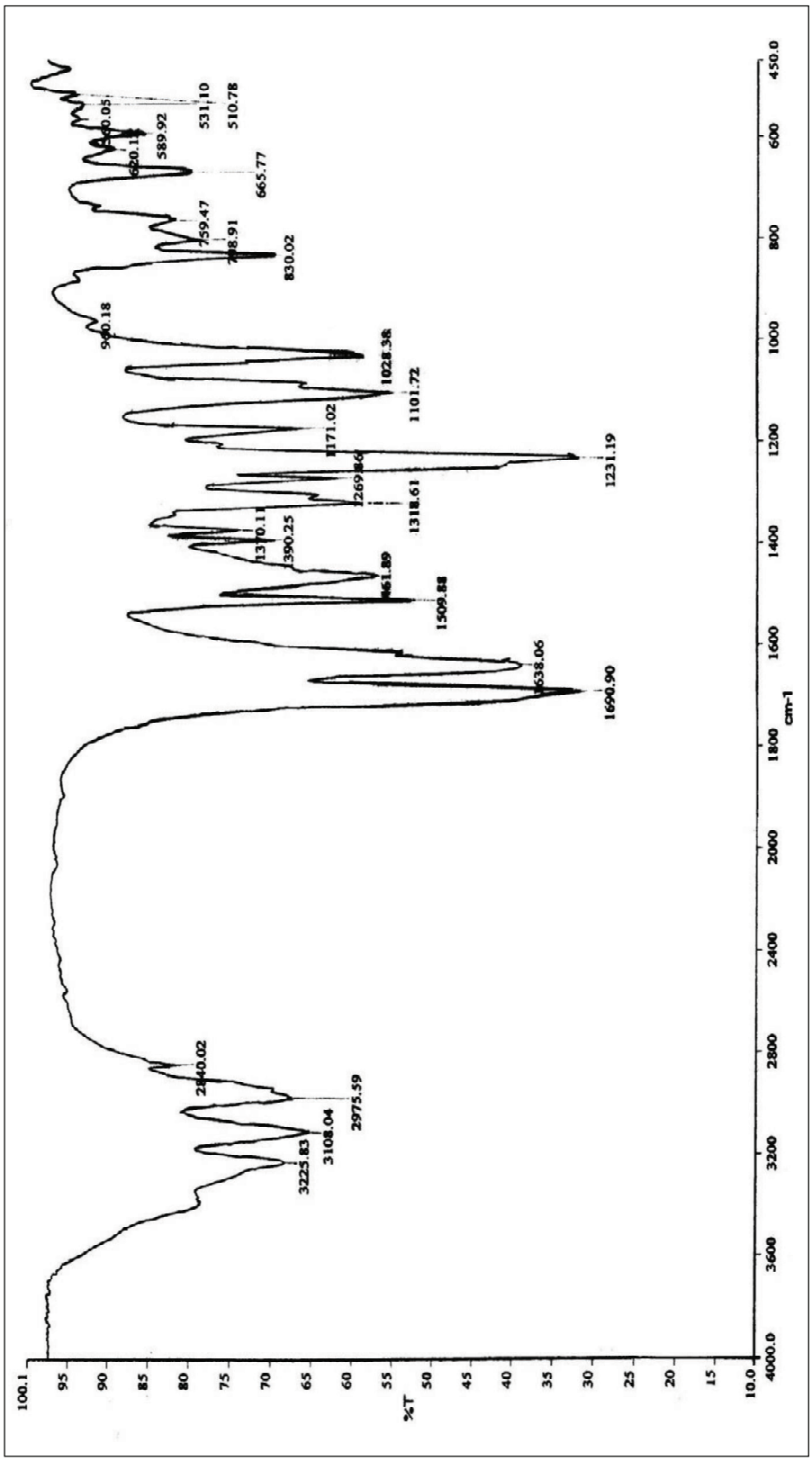

Fig. 4.4: IR spectrum of $[TPAS\text{-}3]_2\,Mn^{+2}$

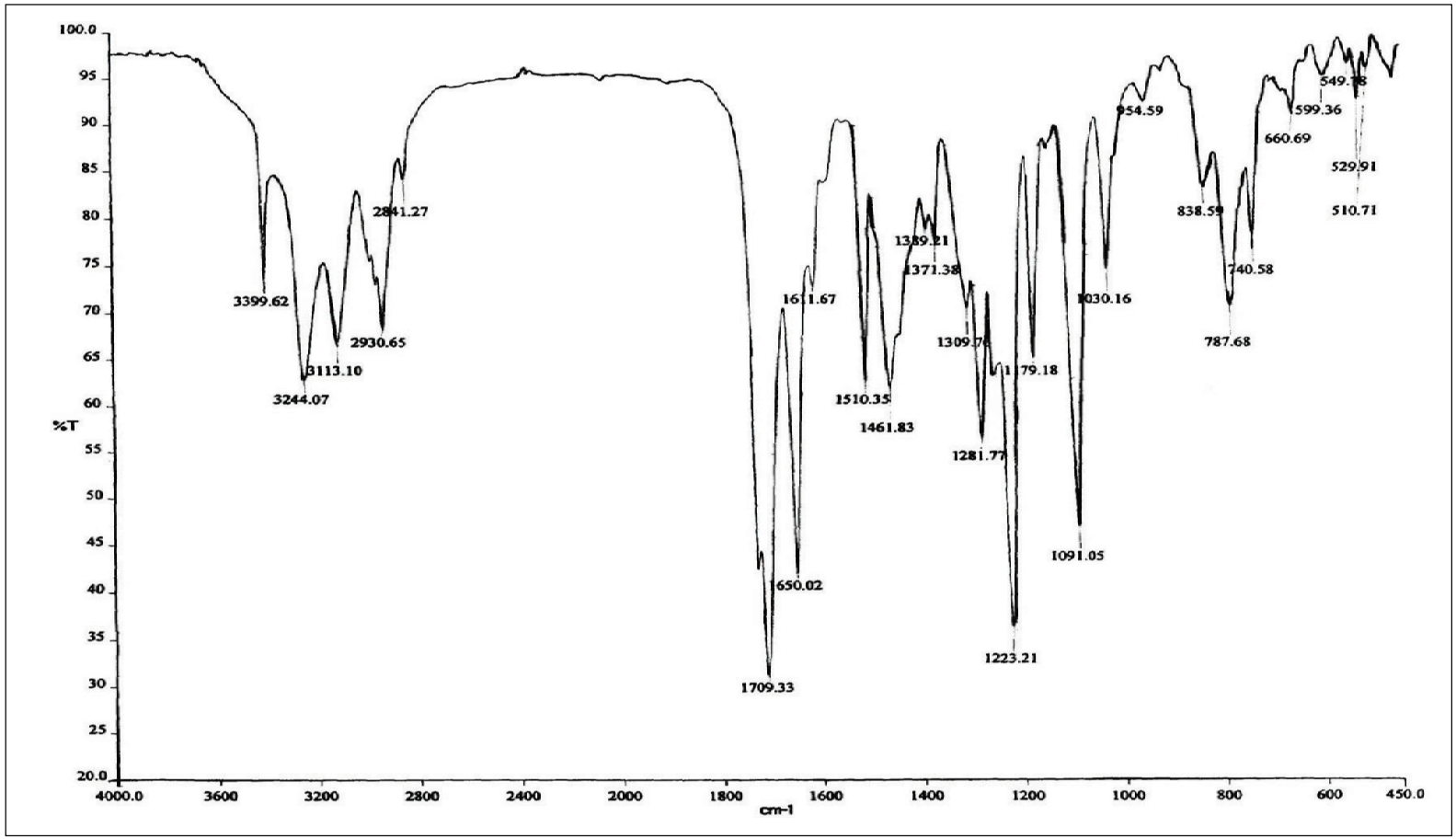

Fig. 4.5: IR spectrum of $[TPAS\text{-}4]_2\ Cu^{+2}$

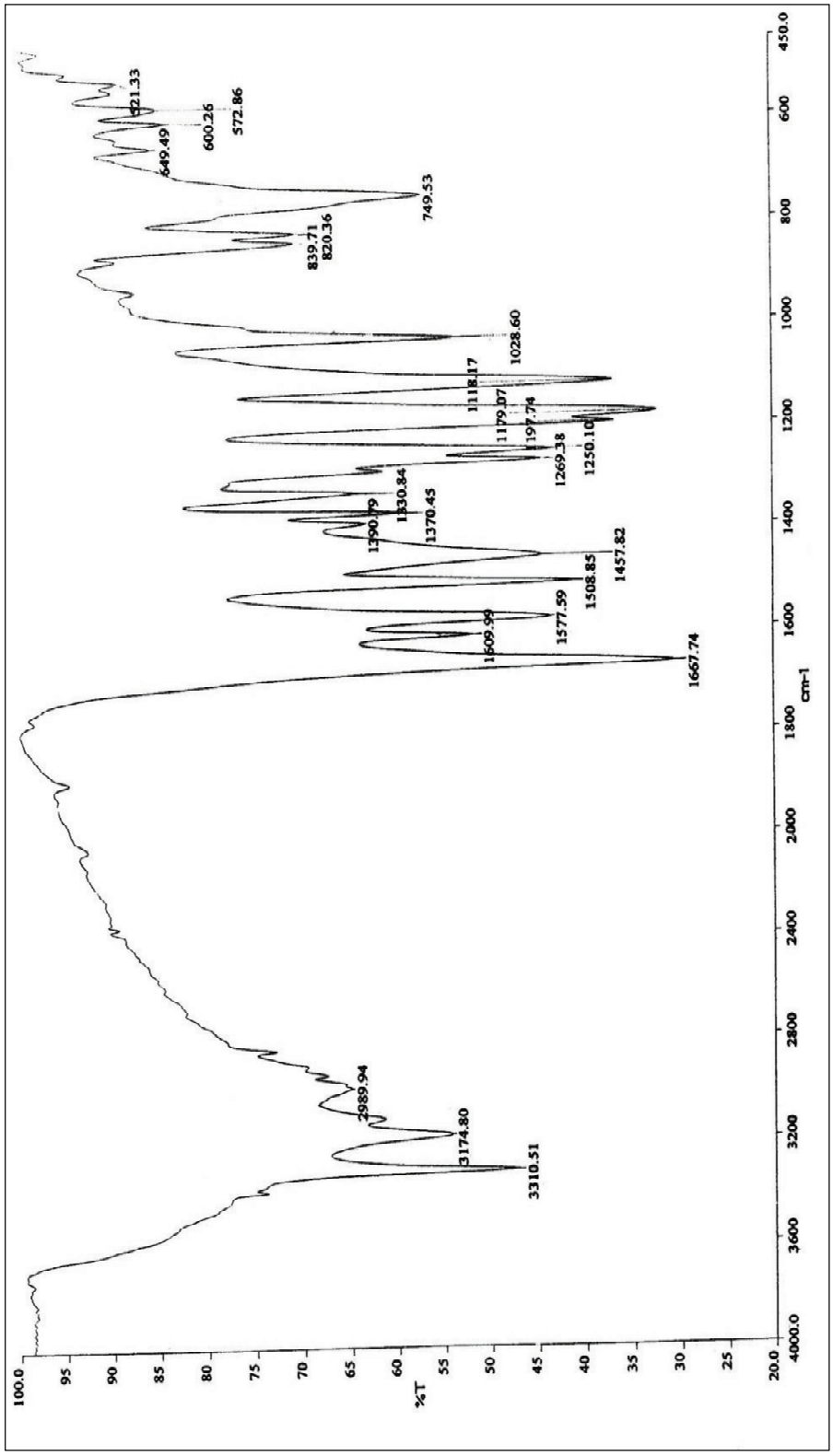

Fig. 4.6: IR spectrum of [TPAS-4]$_2$ Co^{2+}

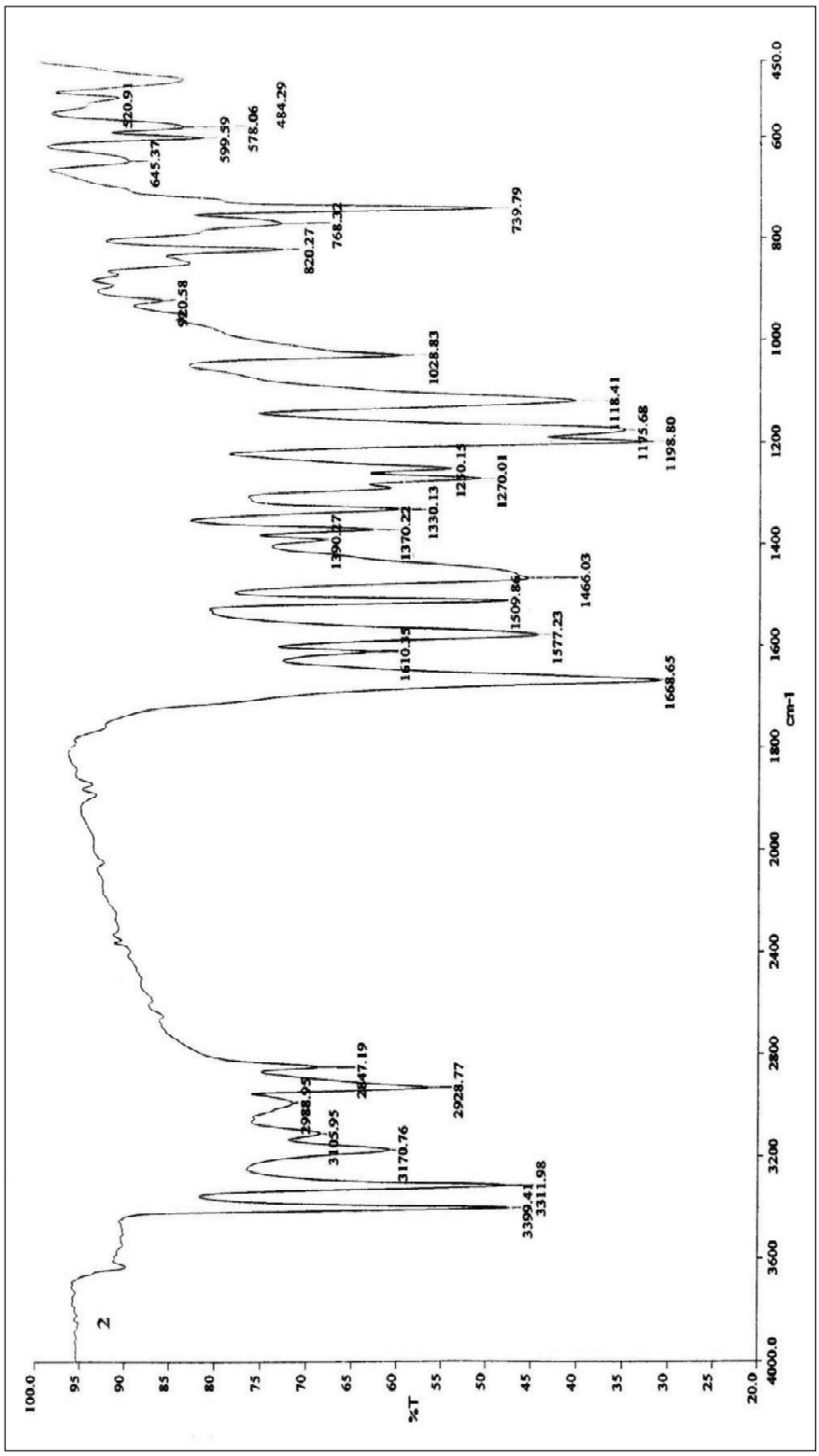

Fig. 4.7: IR spectrum of $[TPAS\text{-}5]_2\ Cu^{2+}$

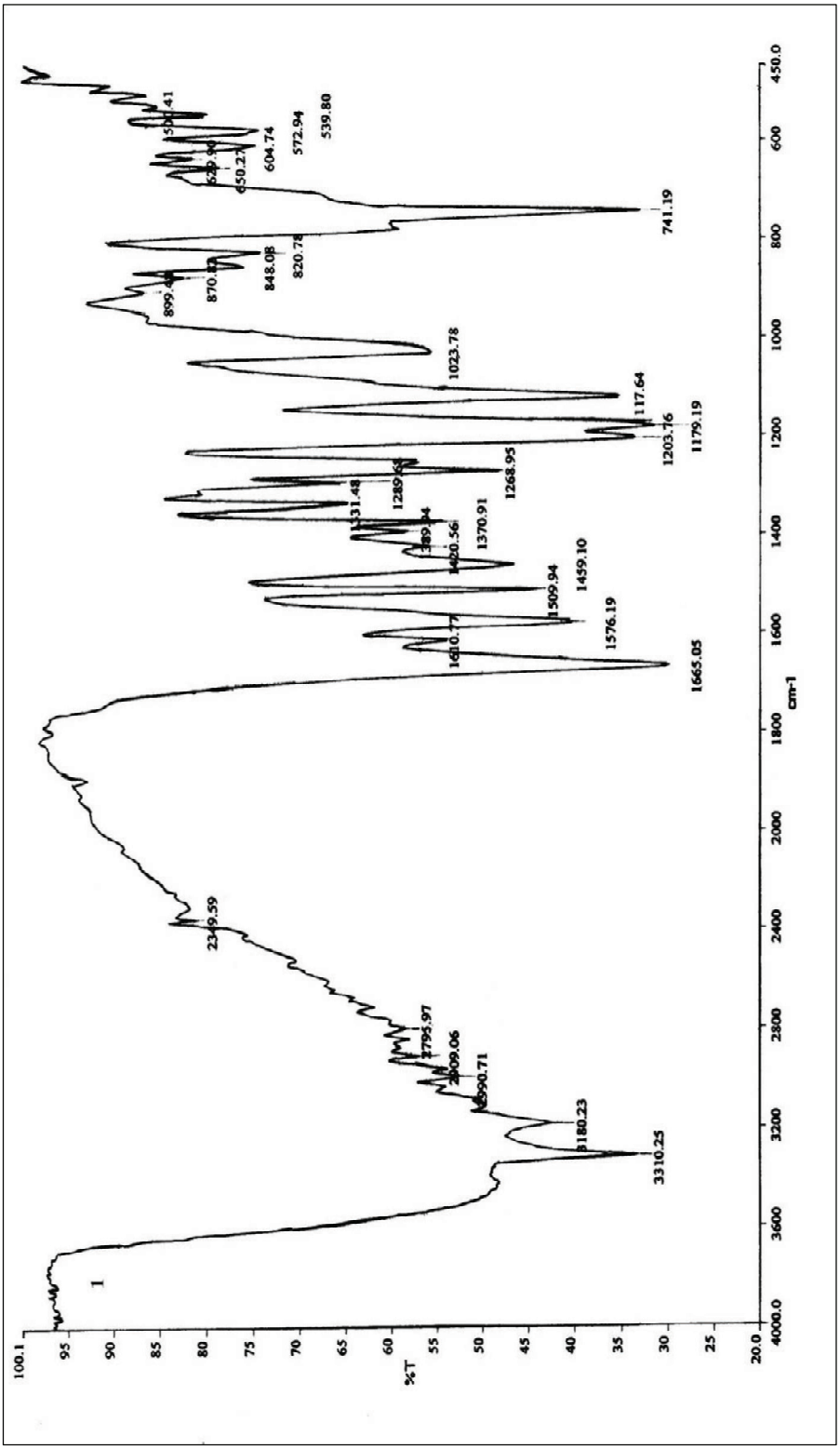

Fig. 4.8: IR spectrum of $[TPTB]_2 Cu^{2+}$

The IR spectra of selected metal chelates are shown in Fig. 4.1 to 4.8.

An inspection of IR spectra of ligands and their corresponding chelates revealed that:

- All the IR spectra have identical bands at their respective positions.
- Most of the bands appeared in the spectra of corresponding ligand are observed at the similar position in the IR spectra of their metal complexes.
- The band due to CO of COOH group appeared in the spectra of ligand is almost absent in the spectrum of complexes.
- The new strong band around 1600 cm^{-1} appeared and this might be responsible for COO^- anion. This is expected as the COOH group of ligand is participating in metal chelate formation.
- Only a new band at 1090-2000 cm^{-1} had appeared in the spectra of metal chelates.
- This may be assigned to V_{C-O} of C-O-Metal bond formation.

As the produced chelates have complex structure, all the bands not appear properly.

4.5 ELECTRONIC SPECTROSCOPY

Electronic (i.e. UV – Visible) spectroscopy is important tool for structural property study of metal chelates. This is for involving.

(i) Solid State properties,

(ii) Stereochemistry,

(iii) Spectral properties

(iv) Photochemistry

(v) Thermal reaction

(vi) Analytical application

All the chelates are in powder forms, so the study has been carried in solid state. Magnesium oxides has been used as reference. Metal chelates may bear four types of transition in the solid spectral region 200 to 800 nm. Wave length.

The two most important types of absorption bands of transition metal chelates in uv-visible region mainly because of metal and ligand and d-d or f-f electron transitions. Kubelka-munk theory[3] can direct the calculation of absorption co-efficient. Many studies have been done based on ligand – field theory[4].

The electronic spectra of all metal produced metal chelates were run on Beckman-Dk-2A spectrophotometer. MgO was used as reference. Spectra of selected samples are presented in Fig. 4.9 to 4.12. Their assignments are included in Table 4.7 to 4.10.

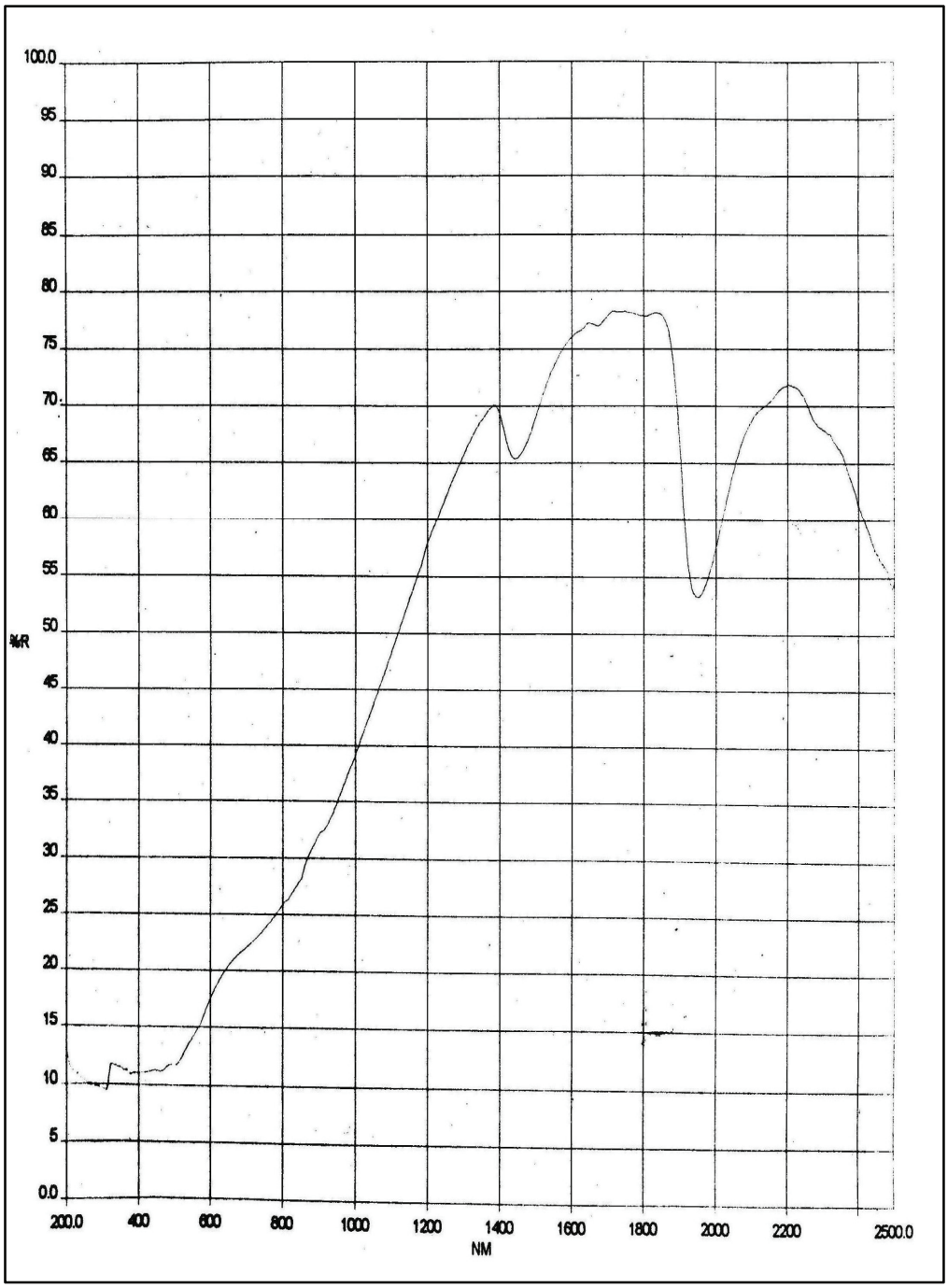

Fig. 4.9: Reflectance spectrum of $(TPAS\text{-}1)_2\text{-}Cu^{2+}$

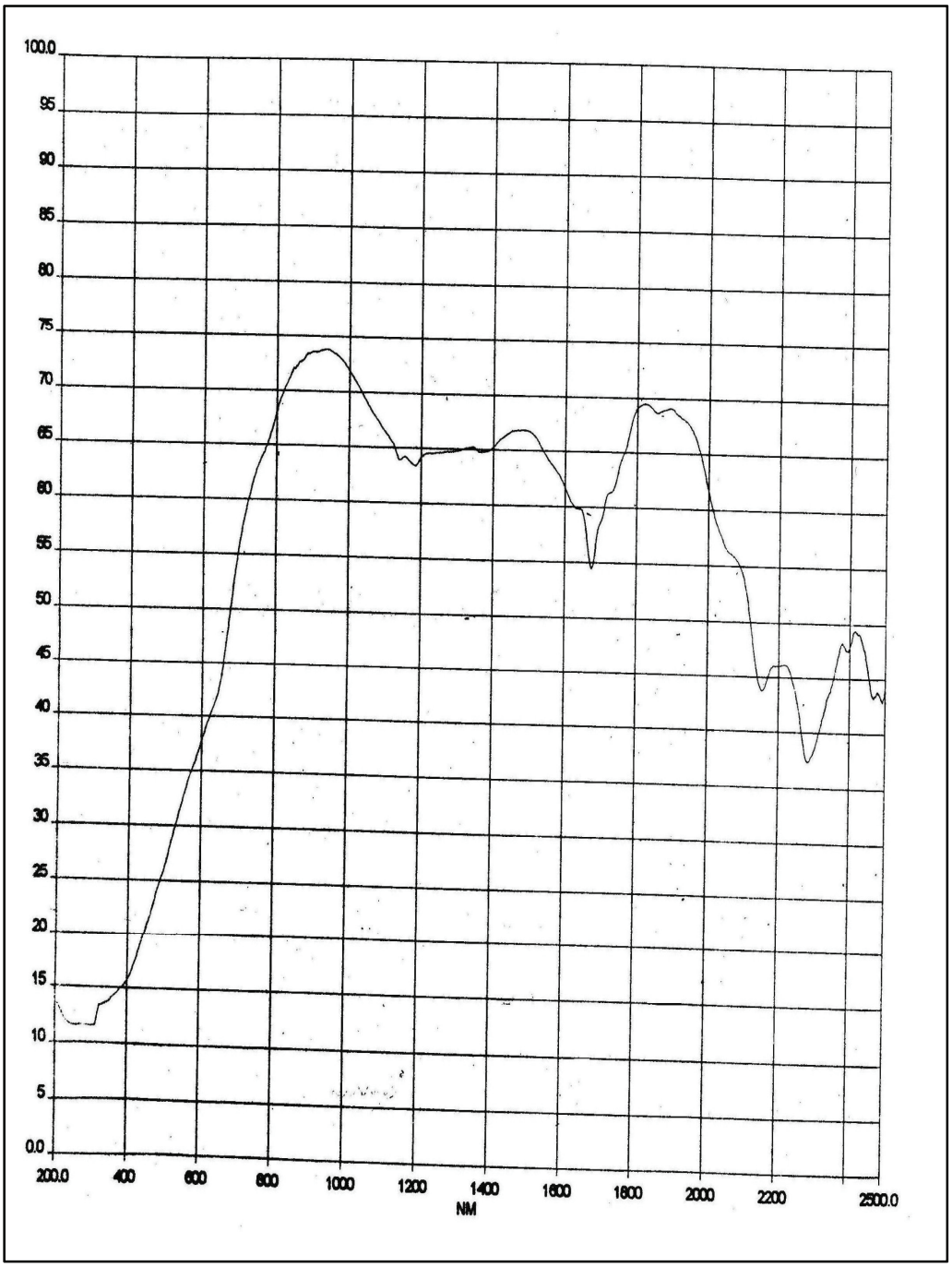

Fig. 4.10: Reflectance spectrum of $(TPAS\text{-}3)_2\text{-}Co^{2+}$

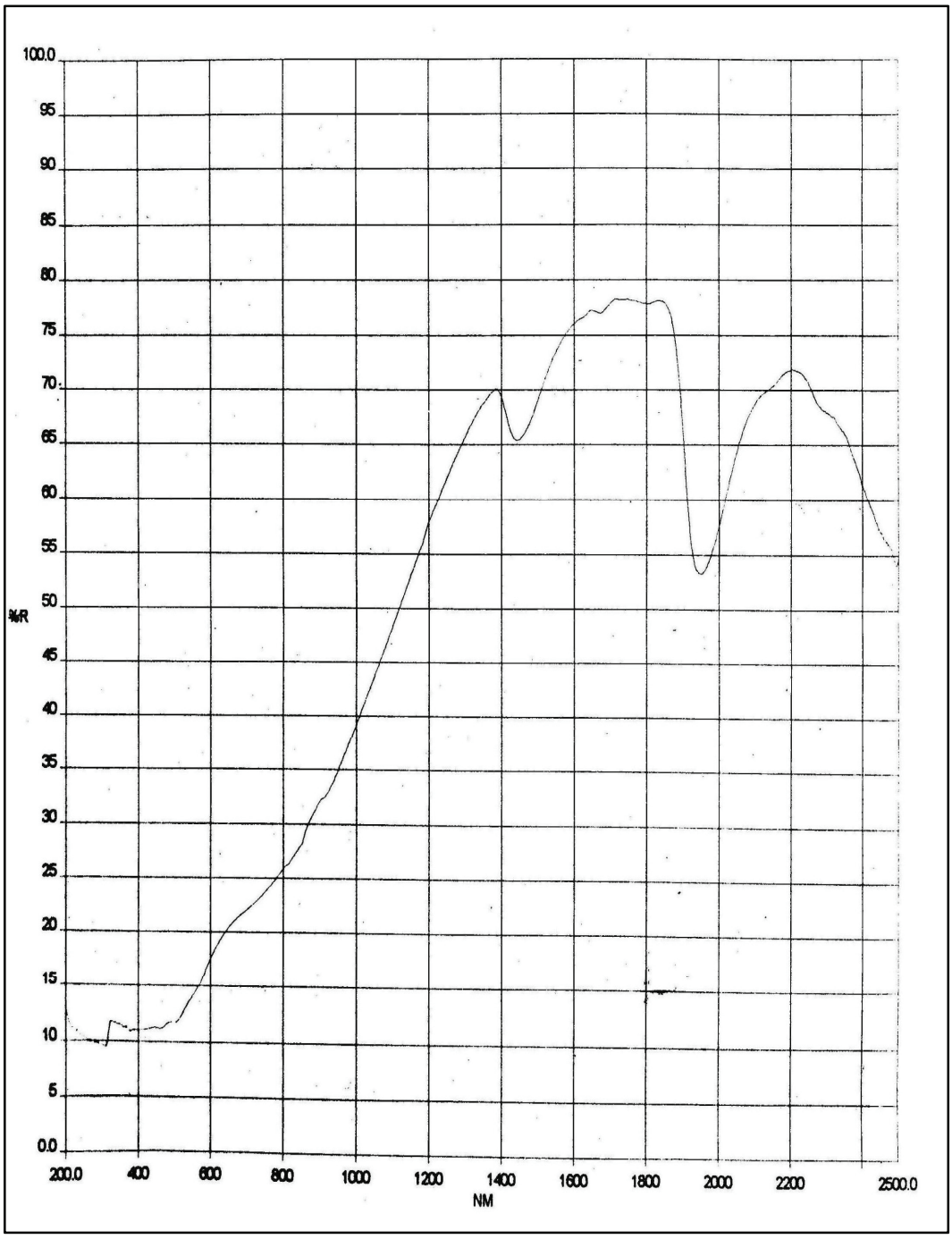

Fig. 4.11: Reflectance spectrum of $(TPAS\text{-}5)_2\text{-}Mn^{2+}$

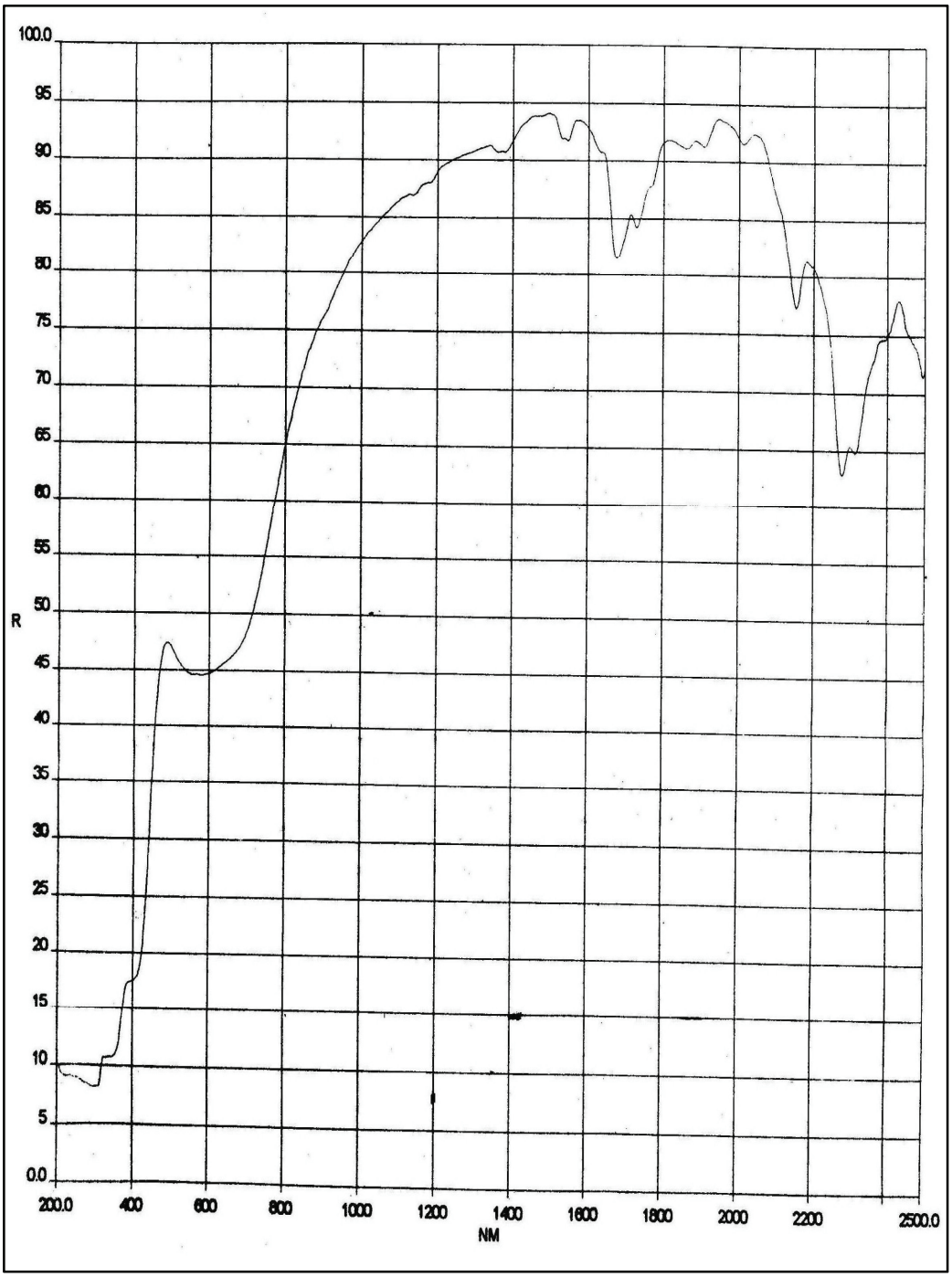

Fig.4.12: Reflectance spectrum of $[TPTB]_2$-Cu^{2+}

Table 4.7: Reflectance spectrum data of Mn^{2+} chelates

Metal Chelates	Observed transition energies (cm^{-1})		
	$^6A_{1g} \rightarrow$		
	$^4A_{1g}$ (4Eg)	$^4T_{2g}$ (4G)	$^4T_{1g}$ (4G)
$(TPAS\text{-}1)_2\ Mn^{2+}$	24030	18650	16215
$(TPAS\text{-}2)_2\ Mn^{2+}$	23880	18340	16845
$(TPAS\text{-}3)_2\ Mn^{2+}$	23980	17643	15460
$(TPAS\text{-}4)_2\ Mn^{2+}$	23415	18592	16122
$(TPAS\text{-}5)_2\ Mn^{2+}$	23785	18411	16723
$(TPTB)_2\ Mn^{2+}$	22125	18535	16100

Table 4.8: Reflectance spectrum data of Co^{2+} Chelates

Metal Chelates	Observed transition energies (cm^{-1})		
	$^4T_{1g}$ (F) $\rightarrow$		
	$^4T_{2g}$ (P)	$^4A_{2g}$	$^4T_{2g}$ (F)
$(TPAS\text{-}1)_2\ Co^{2+}$	24653	19982	8784
$(TPAS\text{-}2)_2\ Co^{2+}$	23956	18116	8743
$(TPAS\text{-}3)_2\ Co^{2+}$	24114	19723	8667
$(TPAS\text{-}4)_2\ Co^{2+}$	22975	19035	8534
$(TPAS\text{-}5)_2\ Co^{2+}$	24933	19893	7421
$(TPTB)_2\ Co^{2+}$	24117	19887	9823

Table 4.9: Reflectance spectrum data of Ni^{2+} Chelates

Metal Chelates	Observed transition energies (cm^{-1})	
	$^3A_{2g} \rightarrow {}^3T_{1g}$ (P)	$^3A_{2g} \rightarrow {}^3T_{1g}$ (F)
$(TPAS\text{-}1)_2\ Ni^{2+}$	24122	15192
$(TPAS\text{-}2)_2\ Ni^{2+}$	22234	15793
$(TPAS\text{-}3)_2\ Ni^{2+}$	22197	14120
$(TPAS\text{-}4)_2\ Ni^{2+}$	22495	13124
$(TPAS\text{-}5)_2\ Ni^{2+}$	22313	15717
$(TPTB)_2\ Ni^{2+}$	24962	14147

Table.4.10: Reflectance spectrum data of Cu^{2+} Chelates

Metal Chelates	Observed transition energies (cm^{-1})	
	CT	$^2B_{1g} \rightarrow {}^2A_{1g}$
$(TPAS\text{-}1)_2\ Cu^{2+}$	23368	15654
$(TPAS\text{-}2)_2\ Cu^{2+}$	23990	15765
$(TPAS\text{-}3)_2\ Cu^{2+}$	24385	15623
$(TPAS\text{-}4)_2\ Cu^{2+}$	24505	15762
$(TPAS\text{-}5)_2\ Cu^{2+}$	24614	14971
$(TPTB)_2\ Cu^{2+}$	23993	15524

4.6 MAGNETIC PROPERTIES

Magnetic behavior of metal chelates is an important property. Thos can be anticipated based on metal and structural unit so for magnetic moment determinedly of metal chelates the two parameter i.e magnetic molar susceptibility (□m) and molecular weight od structural unit are required. The (□m) is defined as what extent the matter is susceptibility magnetic field. There are two types of magnetic field. Paramagnetic and diamagnetic.

Paramagnetic Field: Associated by electron spin and their angular momentum

Diamagnetic Field: Associated by orbital charge particle contribution. This is due to para electrons.

It occurs due to unpaired electron and free radicals. Paramagnetism is inversely proportional to temperature. The compounds having transition metal with unpaired electron are showing and having free radical showing paramagnetism.

Gauy method [5] is useful to determined magnetic susceptibility of metal chelates.

In this method to measure the force created by interactive of applied magnetic field and magnetic moment of the sample (i.e. metal chelates). This force D measured in terms of c (chi) value.

The cylindrical long sample tube with sample D susceptibility in a Gauy balance. The force is measured by applying the magnetic field. The tube constant were determined by using calibrant mercury tetrathicynatocobaltate(II) $Hg[Co(CNS)_4]$.

The mesh powder of metal chelate sample was inserted with tapping till filling Fixed volume. However loose or tight packing of sample does not alter the susceptibility measurements. The tight packing is more desirable for minimizes the orientation changes of particles in the magnetic filed[6]. This tight packing of powder in the tube can be obtained by inserting tiny equale portion of the powder in the tube with end part pounding of each addition. The empty tube was suspendedcin between two magnet pole then weighed. Its apparent weight (w) was noted in presence of magnetic field created by applying 4 and 6 amp electric current[7]. The difference in weight of tube (dw) at both current was noted.

According to Figgis[8] reported that mercury tetrathiocyanatocobaltate (II) $Hg[Co(CNS)_4]$ is best compound to be used as calibrant for magnetic susceptibility measurement. Scientist suggest that this compound is non-volatile, do not absorb moisture and its fine powder has good packing preparation. Its mass magnetic susceptibility (χ_g) is $16.44 \times 10^{-6}(\pm 0.5\%)$ at 20°C. So filling compound into tube the tube constant (shown in equation below) can be calculated. Thus the magnetic moment of unknown compound can be estimate of

$$\chi_g = \frac{\alpha + \beta\, dw_s}{Ws} \qquad \ldots(1)$$

Where

α = Air pocket correction Factor,

β = Tube constants,

Ws = Sample wt in g,

dw_s = Weight difference of the tube filled with sample with magnetic field off and on.

The value of α is estimated using equation

$$\alpha = KV \qquad \ldots(2)$$

Where,

K = Volume of susceptibility of air (0.029×10^{-6} cgs unit), and

V = Volume of air.

The tube constant β is determined at different magnetic field strengths using mercury tetrathiocynatocobaltate (II) as calibrant. The equation used to calculate this constant is:

$$\beta = \chi_r \frac{Wr - KV}{dWr} \quad \ldots(3)$$

Where,

χ_r = Magnetic susceptibility of calibrant(i.e. 16.44 x 10^{-6} cgs ± 0.5 % at 20 ^{0}C)

Wr = Weight (g) of calibrant used in measurement

dWr = Difference in weight (g) of calibrant with and without magnetic field.

K = Volume susceptibility of air (0.029 x 10^{-6} cgs unit), and

V = Volume of air.

The formula (1) is applied to calculate specific susceptibility of sample from the molecule magnetic susceptibility (χ_m) per gram of sample calculated by

$$\chi_m = \chi_g \times Me \quad \ldots(4)$$

Where,

M = Molecular weight of chelate.

The Diamagnetic corrections were made by using pascal's constant[4-7].

$$\chi_{m(corr)} = \chi_m - \text{Pascal's constant} \quad \ldots(5)$$

Finally, the magnetic moment (μ_{eff}) was calculated by formula.

$$\mu_{eff} = \sqrt{(\chi_m')xT} \quad \ldots(6)$$

The unit of μ_{eff} is in Bohr magneton. T is the absolute temperature.

The magnetic moment of all the metal chelates estimated and are presents in Table 4.11 to 4.16.

The Results indicate that the Cu^{+2}, Ni^{2+}, Mn^{2+} and Co^{2+} metal chelates have magnetic moment so these chelates are paramagnetic. However Zn^{2+} metal chelates are diamagnetic as expected. The result μ_{eff} value of each chelates are consistent with theoretical value[8,10].

4.7 MEASUREMENT OF ELECTRICAL CONDUCTIVITY

Conductivity Bridge 305 was used for measuring electrical conductivity of solutions metal complexes in DMF. The value of EC of all the metal chelates are presented in Table 4.11 to 4.16

The specific conductivity of metal chelates were calculated by,

Specific Conductivity = Cell constant x conductivity

$$\text{Molar conductivity} = \text{Sp. Conductivity} \times \frac{1000}{M}$$

M : molarity of the solution.

Table 4.11: Magnetic and conductivity data of metal chelates of ligand TPAS-1

Metal Chelates	**$\chi_g \times 10^{-6}$ (cgs)**	**$\chi_m \times 10^{-6}$ (cgs)**	**Magnetic moment μ_{eff} (BM)**	**$\mu_{eff} = \sqrt{n(n+2)}$ BM**	**μ_{eff} (BM) Expected**	**$\wedge_M^a$**
$(TPAS\text{-}1)_2\ Mn^{2+}$	17.55	14212	5.78	5.91	5.2-6.0	7.21
$(TPAS\text{-}1)_2\ Co^{2+}$	13.45	11125	5.25	3.87	4.4-5.2	19.20
$(TPAS\text{-}1)_2\ Ni^{2+}$	5.65	4760	3.45	2.82	2.9-3.4	9.10
$(TPAS\text{-}1)_2\ Cu^{2+}$	2.10	1815	2.15	1.73	1.7-2.2	7.10
$(TPAS\text{-}1)_2\ Zn^{2+}$	-	-	-	-	D(*)	8.14

Table. 4.12: Magnetic and conductivity data of metal chelates of ligand TPAS-2

Metal Chelates	$\chi_g \times 10^{-6}$ (cgs)	$\chi_m \times 10^{-6}$ (cgs)	Magnetic moment μ_{eff} (BM)	$\mu_{eff} = \sqrt{n(n+2)}$ BM	μ_{eff} (BM) Expected	$\wedge_M^a$
$(TPAS\text{-}2)_2\ Mn^{2+}$	18.54	14676	5.98	5.91	5.2-6.0	7.09
$(TPAS\text{-}2)_2\ Co^{2+}$	14.10	11225	5.20	3.87	4.4-5.2	22.80
$(TPAS\text{-}2)_2\ Ni^{2+}$	5.80	4677	3.35	2.82	2.9-3.4	7.10
$(TPAS\text{-}2)_2\ Cu^{2+}$	2.42	1920	2.14	1.73	1.7-2.2	9.29
$(TPAS\text{-}2)_2\ Zn^{2+}$	-	-	-	-	D(*)	9.81

Table. 4.13: Magnetic and conductivity data of metal chelates of ligand TPAS-3

Metal Chelates	$\chi_g \times 10^{-6}$ (cgs)	$\chi_m \times 10^{-6}$ (cgs)	Magnetic moment μ_{eff} (BM)	$\mu_{eff} = \sqrt{n(n+2)}$ BM	μ_{eff} (BM) Expected	$\wedge_M^a$
$(TPAS\text{-}3)_2\ Mn^{2+}$	17.94	14780	5.97	5.91	5.2-6.0	9.10
$(TPAS\text{-}3)_2\ Co^{2+}$	13.19	10925	5.16	3.87	4.4-5.2	29.10
$(TPAS\text{-}3)_2\ Ni^{2+}$	5.68	4705	3.39	2.82	2.9-3.4	8.20
$(TPAS\text{-}3)_2\ Cu^{2+}$	2.39	1974	2.20	1.73	1.7-2.2	7.98
$(TPAS\text{-}3)_2\ Zn^{2+}$	-	-	-	-	D(*)	10.02

Table 4.14: Magnetic and conductivity data of metal chelates of ligand TPAS-4

Metal Chelates	$\chi_g \times 10^{-6}$ (cgs)	$\chi_m \times 10^{-6}$ (cgs)	Magnetic moment μ_{eff} (BM)	$\mu_{eff} = \sqrt{n(n+2)}$ BM	μ_{eff} (BM) Expected	$\wedge_M^a$
$(TPAS\text{-}4)_2\ Mn^{2+}$	18.55	14782	5.98	5.91	5.2-6.0	5.97
$(TPAS\text{-}4)_2\ Co^{2+}$	14.02	11219	5.20	3.87	4.4-5.2	23.68
$(TPAS\text{-}4)_2\ Ni^{2+}$	5.84	4682	3.38	2.82	2.9-3.4	9.20
$(TPAS\text{-}4)_2\ Cu^{2+}$	2.42	1956	2.19	1.73	1.7-2.2	7.10
$(TPAS\text{-}4)_2\ Zn^{2+}$	-	-	-	-	D(*)	9.62

Table 4.15: Magnetic and conductivity data of metal chelates of ligand TPAS-5

Metal Chelates	$\chi_g \times 10^{-6}$ (cgs)	$\chi_m \times 10^{-6}$ (cgs)	Magnetic moment μ_{eff} (BM)	$\mu_{eff} = \sqrt{n(n+2)}$ BM	μ_{eff} (BM) Expected	$\wedge_M^a$
$(TPAS\text{-}5)_2\ Mn^{2+}$	17.83	14585	5.94	5.91	5.2-6.0	6.72
$(TPAS\text{-}5)_2\ Co^{2+}$	12.90	10635	5.10	3.87	4.4-5.2	28.10
$(TPAS\text{-}5)_2\ Ni^{2+}$	5.40	4435	3.27	2.82	2.9-3.4	9.10
$(TPAS\text{-}5)_2\ Cu^{2+}$	2.32	1888	2.15	1.73	1.7-2.2	4.12
$(TPAS\text{-}5)_2\ Zn^{2+}$	-	-	-	-	D(*)	9.12

Table 4.16: Magnetic and conductivity data of metal chelates of ligand TPTB

Metal Chelates	$\chi_g \times 10^{-6}$ (cgs)	$\chi_m \times 10^{-6}$ (cgs)	Magnetic moment μ_{eff} (BM)	$\mu_{eff} = \sqrt{n(n+2)}$ BM	μ_{eff} (BM) Expected	$\wedge_M^a$
$(TPTB)_2\ Mn^{2+}$	17.54	14733	5.97	5.91	5.2-6.0	7.92
$(TPTB)_2\ Co^{2+}$	13.14	11102	5.21	3.87	4.4-5.2	27.20
$(TPTB)_2\ Ni^{2+}$	5.45	4598	3.36	2.82	2.9-3.4	9.65
$(TPTB)_2\ Cu^{2+}$	2.25	1905	2.16	1.73	1.7-2.2	7.10
$(TPTB)_2\ Zn^{2+}$	-	-	-	-	D(*)	9.12

The data show that metal chelates are less polar in DMF low value i.e < 10 Ω^{-1} cm^2 mol^{-1} of metal chelates indicate that they are non- electrolyte[11].

4.8 MAGNETIC SUSCEPTIBILITY AND REFLECTANCE SPECTRAL DATA CO- RELATION

Cu^{2+} chelates

As electronic configuration Cu^{2+} is $3d^9$ the copper ion containing compounds bear magnetic moment with 1.73 BM value. Theoretical magnetic of copper compounds is in the range of 1.7 to 3.0 BM While the measured μ_{eff} mainly in the range of 1.7 to 2.2 BM. The major Cu^{2+} complexes have tetragonally distorted structure. There are four short co-planer and two longer axial bands, so complexes to be square planer.

Geometrically broad band near 15,000 cm^{-1} is observed so Cu^{2+}chelate have little value for assignment of molecules structure. It was observed that tetragonal distortion is common for Cu^{2+} complex. Two main bands found[12,13]. The energy levels are.

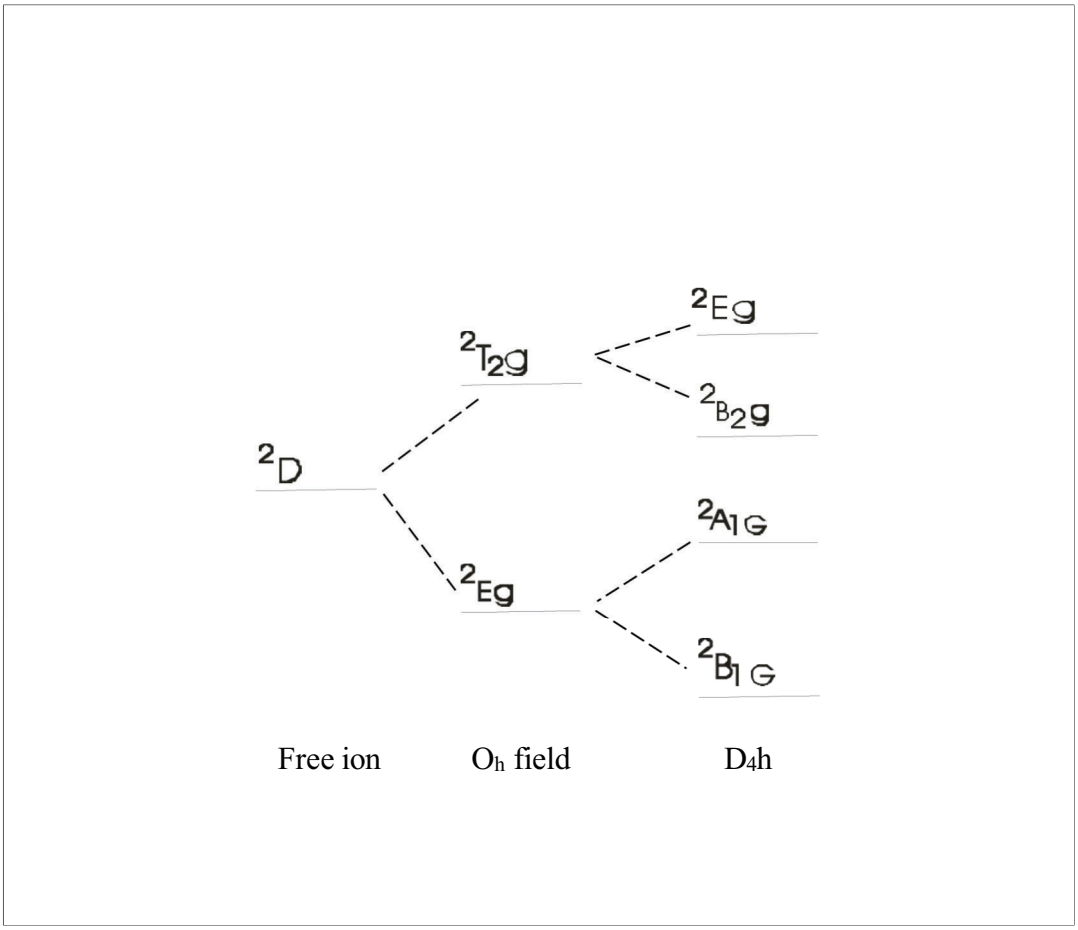

The Cu^{2+} ion in ground state is distorted octahedral field of D_{4h} Symmetry. Its is dx2-y2 (b1g) electron orbital. The transition

$^2B_{1g} \rightarrow {}^2A_{1g}$,

$^2B_{1g} \rightarrow {}^2B_{2g}$

and $^2B_{1g} \rightarrow 2Eg$

assigned tetragonal state. All these exists at

12,000-17,000 cm^{-1}

15,000-18,000 cm^{-1}

and 17,000-20,000 cm^{-1} respectively.

The six co-ordinated Cu^{2+}chelates are distorted octahedral structure (i.e. John – Teller distortion).

In present case (μ_{eff}) of all Cu^{2+} chelates are in the range of 19-20 B.M. This assigned that all Cu^{2+} chelates have distorted octahedral geometry, This also agreed with earlier researchers[14,15].

The bands around 15625–16000 cm^{-1} and 23625–24000 cm^{-1} observed in the reflectance of all Cu^{2+} chelates may attributed to $^2B_{1g} \rightarrow {}^2A_{1g}$ and charge transfer respectively. This also may assigned distorted octahedral geometry for Cu^{2+} chelates.

Ni^{2+} Chelates

There are two unpaired electrons in 3d orbital of Ni^{2+} i.e. Ni^{2+} ($3d^8$). Thus, Ni^{2+} chelates magnetic moment near to spin value for octahedral geometry. Its value of μ_{eff} is high which indicate distorted octahedral chelates. Six co-ordinated Ni^{2+} bears following absorption bands with their transition assignment.

Absorption band cm^{-1}	Transition assignment
7000-13000	$^3A_{2g} \rightarrow {}^3T_{2g}$ (F)
11000-20000	$^3A_{2g} \rightarrow {}^3T_{1g}$ (F)
19000-27000	$^3A_{2g} \rightarrow {}^3T_{1g}$ (P)

In present case the all Ni^{2+} chelates of their μ_{eff} is in the range of 2.9 to 3.4 B.M. Which shoe distorted octahedral geometry. High value of μ_{eff} might be attributed to orbital contribution[16]. The electronic spectra of Ni^{2+} chelates give two bands at 15625 and 22471 Cm^{-1}. May arised from transitions:

$^3A_{1g}(F) \rightarrow {}^3T_{1g}(F)$

and $^3A_{1g}(F) \rightarrow {}^3T_{1g}(P)$

Respectively. This indicated octahedral geometry for all Ni^{2+} chelates.

Table 4.9 show the assignment. The calculations given below

$^3A_{2g} \rightarrow {}^3T_{1g}$ (F) ν_2 $E \approx 18Dq$

$^3A_{2g} \rightarrow {}^3T_{1g}$ (P) ν_3 $E \approx 12Dq + 15B$

It is possible to assign $\nu_2 \approx 15{,}000$ and

$\nu_3 \approx 22{,}000\ cm^{-1}$.

$2\nu_2 = 36Dq = 2 \times 15{,}000$

$= 30{,}000\ cm^{-1}$

$3\nu_3 = 36Dq + 45B$

$= 3 \times 22{,}000$

$= 66{,}000\ cm^{-1}$

$3\nu_3 - 2\nu_2 = 66{,}000 - 30{,}000$

$45B = 36{,}000\ cm^{-1}$

$15B = 12{,}000\ cm^{-1}$

$B = 800\ cm^{-1}$

$12Dq + 15B = 22{,}000\ cm^{-1}$

$12Dq = 22{,}000 - 12{,}000$

$= 10{,}000\ cm^{-1}$

$10Dq = 12{,}000 \times 10 / 12$

$= 10{,}000\ cm^{-1}$

So, these $^3A_{2g} \rightarrow {}^3T_{2g}$ will be 9,166 cm^{-1} in agreement with the reported value in literature for the octahedral Ni^{2+} complexes.

Co^{2+} chelates

Co^{2+} ions have has $3d^7$ electronic configuration. So Co^{2+} chelates have magnetic moment equal to spin only (3.87 B.M). The non generate ground sate increases the spin- only value contributed from higher orbitally degeneration which exists μ_{eff} 4.5 to 5.5 B.M.

The spectra of Co^{2+} due to d-d transition of octahedral species with $^4T_{1g}$ or ^2E_g depends on spin value. The Cu^{2+}chelates in octahedral structure show bands given below[17,18].

	Spectral Range Cm^{-1}	**Transitions**
Near	8000-10000	$^4T_{1g}(F) \rightarrow {}^4T_{2g}(F)$
Far	15000-17000	$^4T_{1g}(F) \rightarrow {}^4T_{2g}(P)$

It is observed that magnitude of magnetic moments lie in the range of 4.4-4.8 BM. These values indicate the possibility of octahedral complexes. Examination of the electronic spectral data reported in table: 4.8 indicate that transitions observed in the range are assigned to transition and another band in the region and may be attributed to and transitions respectively.

Range	**Transition**
8000–9000 cm^{-1}	$^4T_{2g}(F) \rightarrow {}^4T_{1g}(P)$
15625–16650 cm^{-1}	$^4T_{2g}(F) \rightarrow {}^4T_{1g}(P)$
23000 cm^{-1}	$^4T_{2g}(F) \rightarrow {}^4T_{2g}(F)$

So1 based on magnetic moment and spectral Co^{2+} chelates have octahedral geometry as repeated[19,20].

The high spin Co^{2+} chelates are with transition of octahedral structure which are:

$^4T_{1g}$ (F) $\rightarrow$ $^4T_{2g}$ (ν_1) E $\approx$ 8Dq at ~ 8,000 cm^{-1}

$^4T_{1g}$ (F) $\rightarrow$ $^4A_{2g}$ (ν_2) E $\approx$ 18Dq at ~ 16,000 cm^{-1}

and $^4T_{1g}$ (F) $\rightarrow$ $^4T_{1g}$ (P) ν_3 E $\approx$ 6Dq + 15B at ~ 20,000 cm^{-1}

In the present study all the Co^{2+} complexes give three bands in the range at

8000 - 9000 cm^{-1}

19,000 and – 20,000

22,000-25,000 cm^{-1}

Which can be attributed to Above transition. There are shown in Table 4.8

$3\nu_3 - \nu_2 = 3 \times 24,660 - 18,867$

$= 18Dq + 45B - 18Dq$

$= 45B$

$\therefore$ 15B = 18,371 cm^{-1}

ν_3 = 24,660 = 6Dq + 18,371

$\therefore$ Dq = 1048 cm^{-1}

ν_1 = 8Dq = 8385 cm^{-1}

This agrees well with the observed ν_1 value of 8928 cm^{-1}.

Chelates Mn^{2+}

Mn^{2+} chelates are expected to μ_{eff} near to spin only value i.e 5.92 B.M. for unpaired electron in 3d orbital due to oxidation sate of Mn^{2+}ion there are two value of μ_{eff} for Mn^{2+} chelates[21].

Mn^{2+} chelates give the band in 18000–20000 cm^{-1} region and weak band in 23600–24350 cm^{-1} region for octahedral geometry[19].

$^6A_{1g} \rightarrow {}^4T_{1g}(G)$,

$^6A_{1g} \rightarrow {}^4E_{1g}(G)$

and $^6A_{1g} \rightarrow {}^4A_{1g}(G)$ transitions.

In the produced study the magnetic moment (μ_{eff}) of all Mn^{+2} chelates is in the range od 5.5 to 5.9 B.M. The low μ_{eff} value of produced chelates mainly responsible from oxidation of $Mn^{+2} \rightarrow Mn^{+3}$, due to spin exchange. The band exist at 16225 cm^{-1} arised from $^6A_{1g} \rightarrow {}^4T_{1g}(G)$ and second at 24050 cm^{-1} attributed to $^6A_{1g} \rightarrow {}^4T_{2g}(G)$ transition[17].

All these features indicate octahedral geometry. Mn^{+2} has a d^5 orbital so in ground state Mn^{+2} is $^6A_{1g}$. This gives ^4G, ^4D, ^4P, ^4F and ^6S. These terms attributed to field.

$^6S \rightarrow {}^6A_{1g}$

$^4G \rightarrow {}^4A_{1g}, {}^4E_g, {}^4T_{1g}, {}^4T_{2g}$

$^4P \rightarrow {}^4T_{1g}$

$^4F \rightarrow {}^4A_{2g}, {}^4T_{1g}, {}^4T_{2g}$

$^4D \rightarrow {}^4E_g, {}^4T_{2g}$

Metal chelates of Zn^{2+}

Zn^{2+} metal complexes are predicted to show diamagnetic nature as there is no unpaired electron ($3d^{10}$). They have generally tetrahedral geometry[22.]

4.9 THERMOGRAVIMETRIC ANALYSIS

Thermogravimetric analysis of all the metal chelate of all ligands (i.e. of TPAS-1 to TPAS-5 and TPTB) was carried out on Perkin- Elmer Pyris,1 TGA. The TGA data of all the metal chelates are presented in Table- 4.17 to 4.22. Typical TG thermograms are given in Figure 4.13 to 4.15. It was revealed that each complex degrades in two steps. The first stage of decomposition of chelates is in range temperature of 250-500^0 C with a mass loss of about 10%, which indicated the pressure of associated water molecules.

Examination of the TG curves of all the chelates and TG data shown revealed that:

- Each chelate degrades in two steps.
- The degradation of all the chelates start in the temperature range of 200 to 350^{0}C depending upon the natures of chelate.
- The weight loss amount in this first stage is in between 5 to 7 % This may be due to water molecules attached in to the chelates.
- The second stage of decomposition of all chelates is rapid with the loss of mass about 50%. This is due to “in situ” formation of metal oxide during degradation, which accelerated the degradation of chelate.
- The last stage of digression cause a mass loss of about 80%. This is due to loss of molecular fragments of ligand.

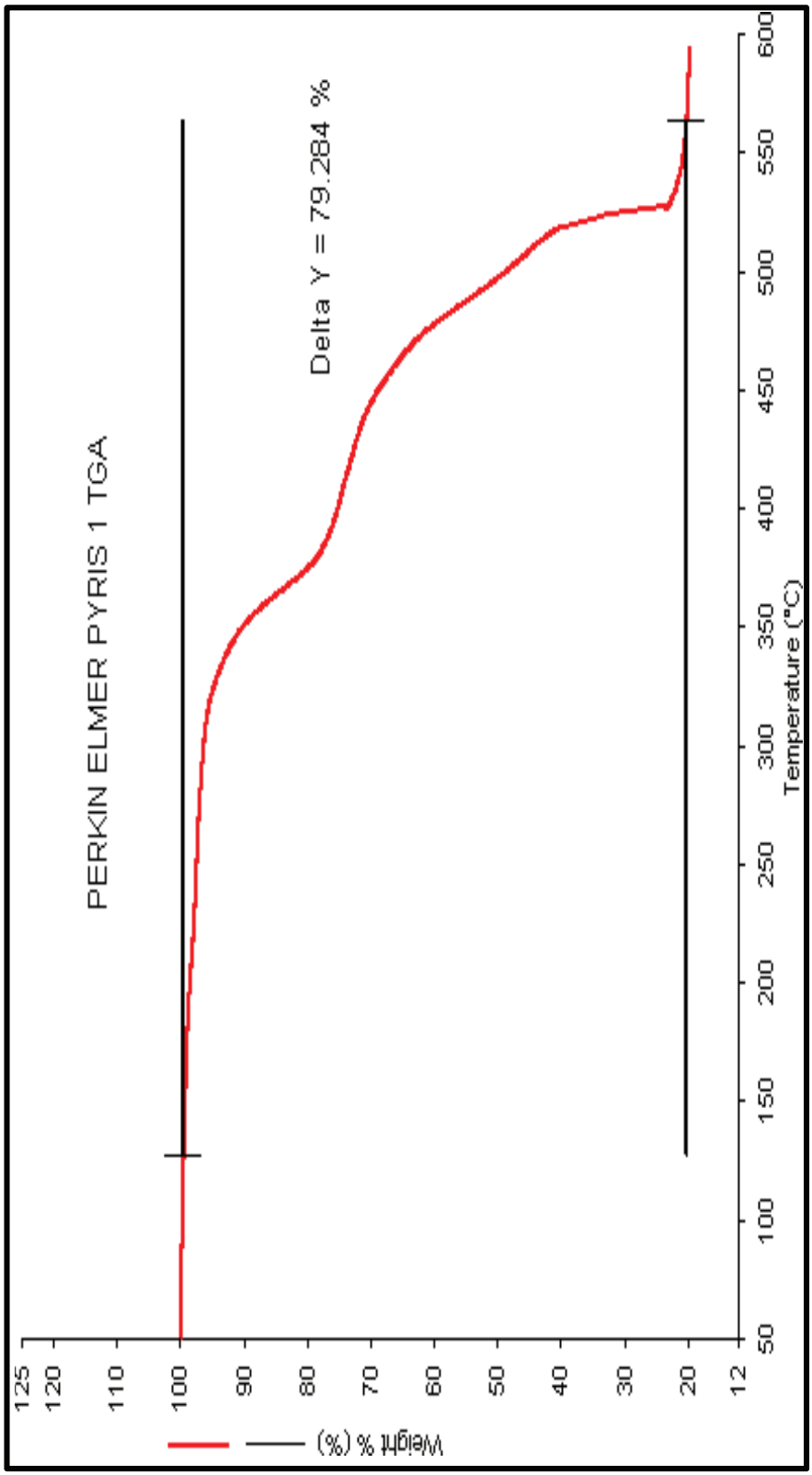

Fig.4.13: TGA thermogram of [TPAS-2] Mn^{2+}

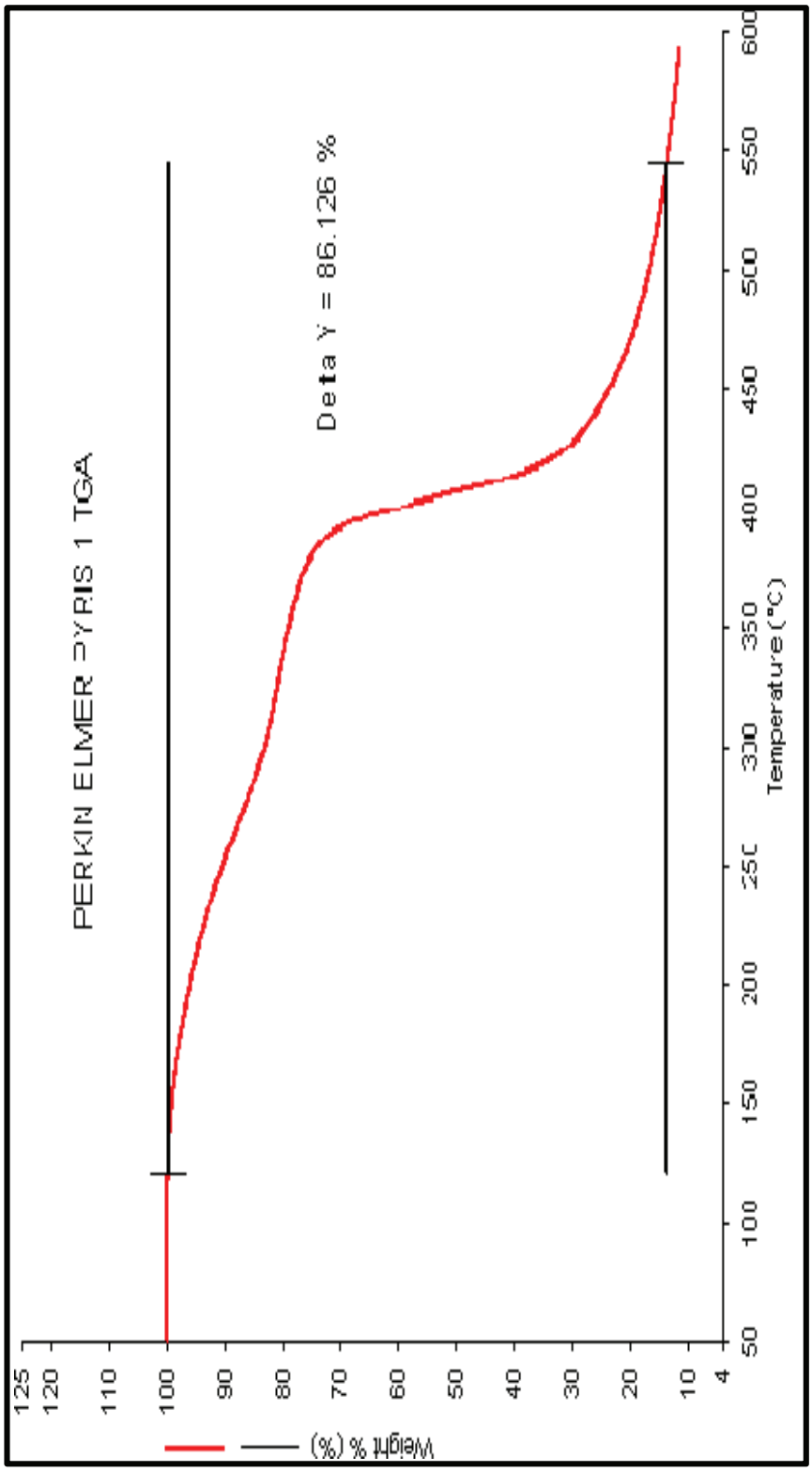

Fig.4.14: TGA thermogram of [TPAS-4] Ni^{2+}

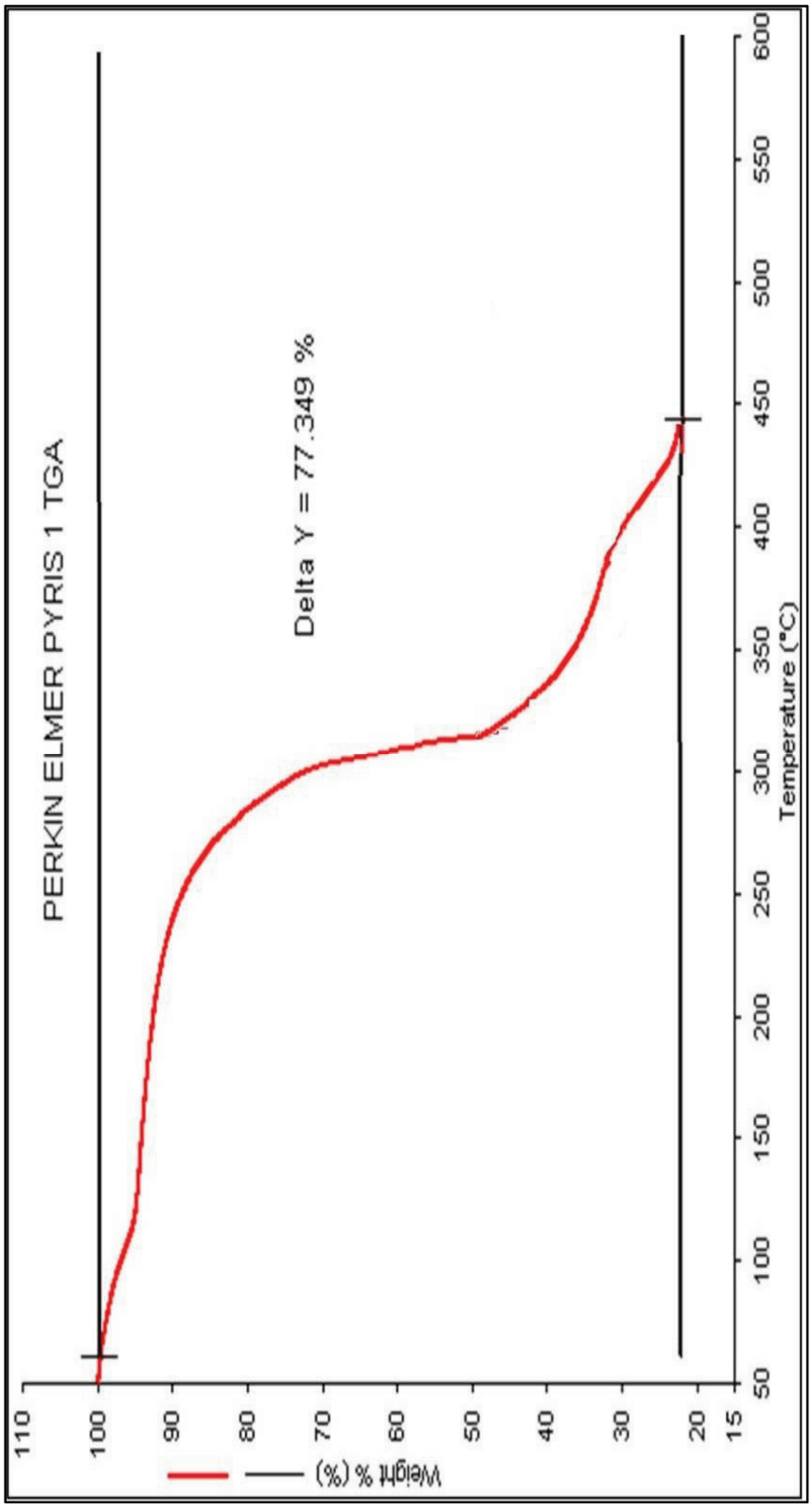

Fig 4.15: TGA thermogram of [TPAS-5] Cu^{2+}

Table 4.17: Thermogravimetric analysis of metal chelates of TPAS-1

Chelate	% Weight loss at temperature (^{0}C)			
	250	**300**	**350**	**400**
[TPAS-1] Cu^{2+}	6.5	7.7	15	29
[TPAS-1] Zn^{2+}	3.2	5.5	25	34
[TPAS-1] Co^{2+}	6.9	14.7	26	36
[TPAS-1] Ni^{2+}	7.6	21	29	42
[TPAS-1] Mn^{2+}	7.9	25.3	32	46

Table 4.18: Thermogravimetric analysis of metal chelates of TPAS-2

Chelate	% Weight loss at temperature (^{0}C)			
	250	**300**	**350**	**400**
[TPAS-2] Cu^{2+}	12.2	17	46	75
[TPAS-2] Zn^{2+}	13	18	50	72
[TPAS-2] Co^{2+}	14	19	55	71
[TPAS-2] Ni^{2+}	15.5	20.5	63	78
[TPAS-2] Mn^{2+}	16.5	22	43	82

Table 4.19: Thermogravimetric analysis of metal chelates of TPAS-3

Chelate	% Weight loss at temperature (^{0}C)			
	250	**300**	**350**	**400**
[TPAS-3] Cu^{2+}	6.7	9.7	62	73
[TPAS-3] Zn^{2+}	5.6	10.4	61	76
[TPAS-3] Co^{2+}	7.7	11	65	73
[TPAS-3] Ni^{2+}	6.6	8	67	72
[TPAS-3] Mn^{2+}	7.8	10.4	66.5	82

Table 4.20: Thermogravimetric analysis of metal chelates of TPAS-4

Chelate	% Weight loss at temperature (^{0}C)			
	250	**300**	**350**	**400**
[TPAS-4] Cu^{2+}	6.4	18.4	22	45
[TPAS-4] Zn^{2+}	11	19.6	24	44
[TPAS-4] Co^{2+}	7.8	18.7	24	51
[TPAS-4] Ni^{2+}	6.7	20.3	25	50
[TPAS-4] Mn^{2+}	8.4	24	28	52

Table 4.21: Thermogravimetric analysis of metal chelates of TPAS-5

Chelate	% Weight loss at temperature (^{0}C)			
	250	**300**	**350**	**400**
[TPAS-5] Cu^{2+}	6.6	9.4	56	68
[TPAS-5] Zn^{2+}	5.6	10.4	61	72
[TPAS-5] Co^{2+}	7.4	11	64	75
[TPAS-5] Ni^{2+}	6.6	10	65	72
[TPAS-5] Mn^{2+}	7.6	10.3	66	77

Table 4.22: Thermogravimetric analysis of metal chelates of TPTB

Chelate	% Weight loss at temperature (^{0}C)			
	250	**300**	**350**	**400**
[TPTB] Cu^{2+}	68	74	78	83
[TPTB] Zn^{2+}	73	75	80	82
[TPTB] Co^{2+}	71	81	84	87
[TPTB] Ni^{2+}	72	75	78	85
[TPTB] Mn^{2+}	76	80	85	91

4.10 ANTIBACTERIAL ACTIVITY

4.10.1 Materials and Methods

(i) All the ligand TPAS-1 to 5 and TPTB and their method chelates have been monitored for antibacterial and antifungal activity.

(ii) Antibacterial activity evaluation:

This was confirmed out by Agra- dise diffusion method. First the culture medium was prepared by talking following investigations.

Peptone: 1.0 g

Sodium Chloride: 0.5 g

Meat Extract (i.e. Beef): 0.3 g

Distilled Water: 100 ml

pH :7.6

Agar: 20 g

The components were dissolved in distilled water and pH was maintained to 7.6 then Agar powder was mixed with it. The syrup was taken in different glass tubes which were plugged by cotton and sterilised at 121^{o}C under 15 lbs /inch pressure for quarter hour. This is called Nutrient Agar Broth (NAB)

(iii) Testing method

This study has been adopted as per method reported. NAB was melted in hot water bath and cooled at 50^{o}C with stirring. It was inoculated by 0.5 – 0.6 ml og fresh bacteria culture (listed below) and mixed well. Then Poured (25ml) in to sterlied each petri dish. The poured material was allowed to set (2 hrs) and then 'wells' were made by punching in to NAB surface by steriled glass rod. Into these wells 0.1 ml of test sample in one solution of test sample in DMF was added by micro pipette. The plates were closed by lids. They kept aside for 7 days, Standard drugs were taken as reference.

Following bacteria have been taken for the study.

Staphylococcus aureus	Gram positive
Streptococcus Pyogenes	Gram positive
Escherrchia	Gram negative
Pseudomonas areuginosa	Gram negative

After seven days the zone of inhibition of growth of bacteria by the test sample was measured in mm. The data are given in Table 4.23 to 4.26.

Chloramphenicol and Ciprofloxacin drugs have been taken as standard (Table 4.23).

Table 4.23: Antibacterial activity of standard drugs

Standard	**Zone of Inhibition* (mm) (activity index)^{std}**			
	Gram positive		**Gram Negative**	
	S. aureus	*S. Pyogenes*	*E. Coli*	*P. aeruginosa*
Chloramphenicol	22	23	29	21
Ciprofloxacin	19	21	23	24

Antifungal activity of standard drugs

Standard	Zone of Inhibition* (mm) (activity index)^{std}	
	C. albicans	*A. Niger*
Nystatin	20	23
Greseofulvin	27	27

* = average zone of inhibition in mm,

Activity index = Inhibition zone of the sample / Inhibition zone of the standard

Table 4.24: Antibacterial activity of ligands TPAS-1, TPAS-2 and their metal chelates.

Sample	Zone of inhibition* (mm) (Activity index)[std]			
	Gram Positive		Gram Negative	
	S. aureus	*S. Pyogenus*	*E. Coli*	*P. aeruginosa*
TPAS-1	08	09	11	11
$(TPAS\text{-}1)_2\ Cu^{2+}$	14	15	15	17
$(TPAS\text{-}1)_2\ Mn^{2+}$	14	12	15	11
$(TPAS\text{-}1)_2\ Co^{2+}$	13	12	15	13
$(TPAS\text{-}1)_2\ Zn^{2+}$	18	17	14	16
$(TPAS\text{-}1)_2\ Ni^{2+}$	21	16	13	18
TPAS-2	11	10	08	09
$(TPAS\text{-}2)_2\ Cu^{2+}$	10	13	12	17
$(TPAS\text{-}2)_2\ Mn^{2+}$	14	09	13	17
$(TPAS\text{-}2)_2\ Co^{2+}$	16	17	11	16
$(TPAS\text{-}2)_2\ Zn^{2+}$	18	21	11	16
$(TPAS\text{-}2)_2\ Ni^{2+}$	11	16	18	19

Table 4.25: Antibacterial activity of ligands TPAS-3, TPAS-4 and their metal chelates.

Sample	Zone of inhibition* (mm) (Activity index)^{std}			
	Gram Positive		Gram Negative	
	S. aureus	*S. Pyogenus*	*E. Coli*	*P. aeruginosa*
TPAS-3	11	10	08	11
$(TPAS\text{-}3)_2\ Cu^{2+}$	16	19	17	18
$(TPAS\text{-}3)_2\ Mn^{2+}$	13	14	15	13
$(TPAS\text{-}3)_2\ Co^{2+}$	17	14	16	17
$(TPAS\text{-}3)_2\ Zn^{2+}$	14	15	16	18
$(TPAS\text{-}3)_2\ Ni^{2+}$	14	17	14	15
TPAS-4	17	18	18	20
$(TPAS\text{-}4)_2\ Cu^{2+}$	21	20	21	22
$(TPAS\text{-}4)_2\ Mn^{2+}$	18	20	19	21
$(TPAS\text{-}4)_2\ Co^{2+}$	22	21	21	18
$(TPAS\text{-}4)_2\ Zn^{2+}$	20	20	23	20
$(TPAS\text{-}4)_2\ Ni^{2+}$	21	18	18	19

Table 4.26: Antibacterial activity of ligands TPAS-5 and TPTB and their metal chelates.

Sample	Zone of inhibition* (mm) (Activity index)^{std}			
	Gram Positive		Gram Negative	
	S. aureus	*S. Pyogenus*	*E. Coli*	*P. aeruginosa*
TPAS-5	12	11	10	11
$(TPAS\text{-}5)_2\ Cu^{2+}$	11	10	12	13
$(TPAS\text{-}5)_2\ Mn^{2+}$	15	15	11	09
$(TPAS\text{-}5)_2\ Co^{2+}$	17	18	16	14
$(TPAS\text{-}5)_2\ Zn^{2+}$	21	18	16	15
$(TPAS\text{-}5)_2\ Ni^{2+}$	20	20	20	20
TPTB-5	08	10	11	09
$(TPTB)_2\ Cu^{2+}$	11	16	12	16
$(TPTB)_2\ Mn^{2+}$	18	09	15	14
$(TPTB)_2\ Co^{2+}$	10	10	08	08
$(TPTB)_2\ Zn^{2+}$	12	13	12	11
$(TPTB)_2\ Ni^{2+}$	10	07	14	16

4.11 ANTIFUNGAL ACTIVITY

For monitoring the antifungal activity of all the produced samples was carried out by using plant pathogens. These are:

(a) C. albicans

(b) A. Nigar

The antifungal activity of all the ligand and their metal chelates was evaluated

at 1000 ppm concentration of wave plant pathogens. Each of these fungus inoculated on steriled potato dextrose. Agar (PDA) medium in a pre- steriled petri dish (PDA prepared from 200 g Potato, 20 g Dextrose and 20 g of Agar and water 1 lit). Thus test sample was added in petri dish and then auto cooked 120ºC for 15 min under 15 lb/inch pressure. The petri dish were closed and kept for seven days. After the zone of inhibition were measure in percentage by formula,

$$\text{Zone of inhibition \%} = \left(\frac{A - B}{A}\right) \times 100$$

Where A : Area of colony control play

B : Area of colony in test play

The result are shown in Table 4.27 to 4.29.

Table 4.27: Antifungal activity of ligand TPAS-1, TPAS-2 and their metal chelates

Sample	Zone of inhibition (mm) (activity index)[std]	
	C. albicans	***A. Niger***
TPAS-1	07	10
$(TPAS\text{-}1)_2\ Cu^{2+}$	19	21
$(TPAS\text{-}1)_2\ Mn^{2+}$	18	20
$(TPAS\text{-}1)_2\ Co^{2+}$	17	19
$(TPAS\text{-}1)_2\ Zn^{2+}$	18	21
$(TPAS\text{-}1)_2\ Ni^{2+}$	17	18
TPAS-2	10	11
$(TPAS\text{-}2)_2\ Cu^{2+}$	16	17
$(TPAS\text{-}2)_2\ Mn^{2+}$	18	18
$(TPAS\text{-}2)_2\ Co^{2+}$	11	13
$(TPAS\text{-}2)_2\ Zn^{2+}$	13	16
$(TPAS\text{-}2)_2\ Ni^{2+}$	17	18

Table 4.28: Antifungal activity of ligand TPAS-3, TPAS-4 and their metal chelates

Sample	Zone of inhibition (mm) (activity index)^{std}	
	C. albicans	***A. Niger***
TPAS-3	08	11
$(TPAS\text{-}3)_2\ Cu^{2+}$	18	19
$(TPAS\text{-}3)_2\ Mn^{2+}$	17	21
$(TPAS\text{-}3)_2\ Co^{2+}$	16	18
$(TPAS\text{-}3)_2\ Zn^{2+}$	20	18
$(TPAS\text{-}3)_2\ Ni^{2+}$	18	18
TPAS-4	08	12
$(TPAS\text{-}4)_2\ Cu^{2+}$	17	17
$(TPAS\text{-}4)_2\ Mn^{2+}$	16	18
$(TPAS\text{-}4)_2\ Co^{2+}$	13	15
$(TPAS\text{-}4)_2\ Zn^{2+}$	16	14
$(TPAS\text{-}4)_2\ Ni^{2+}$	16	13

Table 4.29: Antifungal activity of ligand TPAS-5, TPTB and their Metal chelates.

Sample	Zone of inhibition (mm) (activity index)[std]	
	C. albicans	*A. Niger*
TPAS-5	10	11
$(TPAS\text{-}5)_2\ Cu^{2+}$	18	17
$(TPAS\text{-}5)_2\ Mn^{2+}$	19	20
$(TPAS\text{-}5)_2\ Co^{2+}$	18	18
$(TPAS\text{-}5)_2\ Zn^{2+}$	20	19
$(TPAS\text{-}5)_2\ Ni^{2+}$	18	19
TPTB	09	12
$(TPTB)_2\ Cu^{2+}$	15	18
$(TPTB)_2\ Mn^{2+}$	17	19
$(TPTB)_2\ Co^{2+}$	13	14
$(TPTB)_2\ Zn^{2+}$	15	13
$(TPTB)_2\ Ni^{2+}$	18	11

4.12 CONCLUSION

In the present study, sulfa drug containing ligands were prepared. The ligands were proposed by simple condensation of tetrahydrophthalic anhydride and various sulfa drugs. Five simple ligands and one bis ligands were prepared and characterised on the basis of elemental analysis, spectral studies. thermogravimetric analysis and C, H, N, S-content. IR/NMR spectral features of all the ligands are almost identical with slight variation of group frequency and type of proton. The LC-MS data give the molecular mass peak for ligands. All these facts confirmed the structure of ligands. The thermogravimetric analysis of all the ligand support carboxylic group, which on thermal degradation eliminates CO_2 gas. Such degradation of ligand was shown in thermogram, which agree with theoretical value.

Metal complexes of Cu^{2+}, Ni^{2+}, Co^{2+}, Mn^{2+} and Zn^{2+}metal ions with each ligand were synthesized. All the metal complexes are insoluble in water and common organic solvents. All the metal complexes suggest that M:L ratio is 1:2 while that of metal complexes of bis ligand suggest M:L ratio is 1:1.

IR spectra of all the metal complexes of each series are almost identical in terms of all aspects, only discernible difference is observed in IR spectra of metal complexes. The broad band due to OH of COOH in the region 4000-2500 cm^{-1} was narrowing due to coordination bond formation of COOH with metal ion. However, the narrowing band may be due to coordinated water molecule. The new band due to M-O was observed. The band due to C=O group of COOH in the ligand is almost vanished and the new band due to COO^- anion appeared. These IR spectral features confirm the metal complexation.

Thermal degradation of all the metal complexes suggest that each complex degrade initially due to associated water. Then rapid degradation due to *in situ* acceleration by metal oxide formation during thermal degradation.

The magnetic moment and reflectance spectra of all the metal complexes suggest geometry of each type of ligand. The results suggested that $Cu^{2+}$and Ni^{2+} metal complexes have tetrahedral geometry and paramagnetic. The Co^{2+} and Mn^{2+} complexes have octahedral geometry and paramagnetic. As expected, Zn^{2+} metal complexes are diamagnetic.

The results of antimicrobial activity of all the ligands and their metal complexes indicated that all these compounds are more or less toxic against bacteria and fungi. The results show that the Cu^{2+} metal complexes are more toxic.

❐❐❐

REFERENCES

[1] A. I. Vogel, A Textbook of Quantitative Chemical Analysis Revised by J. Bessett, R. C. Denny, J. H. Feffery and J. Mondhaus. ElBS, 5th Edition, Pearsons, Indian edition (2004).

[2] R. A. Ahmadi and S. Amani**,** Synthesis, Spectroscopy, Thermal Analysis, Magnetic Properties and Biological Activity Studies of Cu(II) and Co(II) Complexes with Schiff Base Dye Ligands Molecules, **17**(6), 6434-6448 (2012).

[3] H. A. Bayoumi, A. Alaghaz, and M. Aljahdali, Cu(II), Ni(II), Co(II) and Cr(III) Complexes with N2O2- Chelating Schiff's Base Ligand Incorporating Azo and Sulfonamide Moieties: Spectroscopic, Electrochemical Behavior and Thermal Decomposition Studies. Int. J. Electrochem. Sci., **8**, 9399-9413 (2013).

[4] S. L. Simmons, The application of diffuse reflectance spectroscopy to the chemistry of transition metal coordination compounds**.** Co-ord. Chem. Rev., **14**(2), 181-196 (1974).

[5] L. N. Mulay, Magnetic Susceptibility, John willey and sons, interscience Publishers, New York (1972).

[6] G. Kortum and H. Schoter, The acquisition of quantitative absorption spectra of solid substances in reflection. Z. Naturforsch, **2a**, 652-657 (1947).

[7] G. Kortum and H. Schoter, Z. Electrochem., 57, 353 (1953).

[8] B. N. Figgis, The magnetochemistry of complexes in modern Coordination chemistry. Interscience, NewYork, 403-406 (1960).

[9] H. A. Bayoumi and A. N. Alaghaz, Cu(II), Ni(II), Co(II) and Cr(III) Complexes with N2O2- Chelating Schiff's Base Ligand Incorporating Azo and Sulfonamide Moieties: Spectroscopic, Electrochemical Behavior and Thermal Decomposition Studies. Int. J. Electrochem. Sci., **8**, 9399-9413 (2013).

[10] E. L. Simmons, The application of diffuse reflectance spectroscopy to the chemistry of transition metal coordination compounds. Co-ord. Chem. Rev., **14**(2), 181-196 (1974).

[11] R. A. Ahmadi, And S. Amani, Synthesis, Spectroscopy, Thermal Analysis, Magnetic Properties and Biological Activity Studies of Cu(II) and Co(II)

Complexes with Schiff Base Dye Ligands**.** Molecules, **17**(6), 6434- 6448 (2012).

[12] P. S. N. Reddy and B. V. Agarwala, Synthesis and Characterization of New Schiff Base Complexes of 2-Pyridinecarboxaldehyde and Thiosemicarbazides. Syn. React. Inrg. Chem., **17**, doi.10.1080/00945718708059456 (1987).

[13] A. K. Patel, V. M. Patel, R. M. Patel, S. Singh and J. D. Joshi, Synthesis, Characterization and Antimicrobial Activities of Ni(II), Cu(II), Zn(II) and Cd(II) Ternary Complexes Involving 8-Quinolinol as Primary Ligand and Bidentate Glycine or Tridentate Aspartic Acid as Secondary Ligand. Synth. React. Inorg. Met. Org. Chem., **29**(2), doi.10.1080/00945719909349443 (1999).

[14] C. K. Jorgenson, Comparative Crystal Field Studies of some Ligands and the Lowest Singlet State of Paramagnetic Nickel(II) Complexes. Acta. Chem. Scand., **9**, 1362-1377 (1955).

[15] D. C. Patel and P. K. Bhattacharya, Studies in some Ni(II) and Cu(II) complexes. J. Ind. Chem. Soc., **49**, 1041-1043 (1972).

[16] J. Lewis and R. S. Wilkins, Modern Coordination chemistry, New york, 290 (1960).

[17] B. Sing and R. Sing, Transition metal complexes of 3-(4-pyridyl)-triazoline-5-thione J. Inorg. Nucl. Chem., **34**(11), 3449-3454. (1972).

[18] B. Sing and U. Agarwal, Transition metal complexes of 1-substituted tetrazoline-5-thiones. J. Inorg. Nucl. Chem., **8**, 2515-2525 (1969).

[19] S. Satpathi, H. C. Rai and B. S. Sahoo, Antiferromagnetic spincoupling in low spin cobalt(II) and medium spin manganese (II) dimers. J. Ind. Chem. Soc., **52**, 701 (1975).

[20] P. K. Patel and P. D. Patel, Synthesis, Characterization, Metal Complexation Studies and Biological screening of some Newly Synthesized Metal Complexes of 1-(4-carboxy-3-hydroxy-N-isopropyl phenyl amino methyl)

benzotriazole with Some Transition Metals. Int. J. of Chem Tech. research, **2**(2), 1147-1152 (2010).

[21] P. R. Reddy, M. Radhika, and P Manjula, Synthesis and characterization of mixed ligand complexes of Zn(II) and Co(II) with amino acids: Relevance to zinc binding sites in zinc fingers. J. Chem. Sci., **117** (3), 239-246 (2005).

[22] A. V. Nikolav, V. A. Logvineko and L. T. Mychina, Thermal Analysis, Academic Press, New York, **2**, 779 (1969).

❐❐❐